UNITED STATES DEPARTMENT OF THE INTERIOR

GEOLOGICAL SURVEY

Seismic Measurements of Explosions in the Tatum Salt Dome, Mississippi

by

R. D. Borcherdt, J. H. Healy, W. H. Jackson
and D. H. Warren

1967

Open-file report 67-24

UNITED STATES
DEPARTMENT OF THE INTERIOR
GEOLOGICAL SURVEY

SEISMIC MEASUREMENTS OF EXPLOSIONS IN THE TATUM SALT DOME, MISSISSIPPI

by

R. D. Borcherdt, J. H. Healy, W. H. Jackson, and D. H. Warren

INTRODUCTION

Project Sterling provided for the detonation of a nuclear device in the cavity resulting from the Salmon nuclear explosion in the Tatum salt dome in southern Mississippi (Figure 1). It also provided for a high explosive (HE) comparison shot in a nearby drill hole.

The purpose of the experiment was to gather information on the seismic decoupling of a nuclear explosion in a cavity by comparing seismic signals from a nuclear shot in the Salmon cavity with seismic signals recorded from Salmon and with seismic signals recorded from a small (about 2 tons) HE shot in the salt dome. Surface seismic measurements were made by the U. S. Geological Survey, the U. S. Coast and Geodetic Survey, and the Air Force Technical Applications Center with coordination and overall direction by the Lawrence Radiation Laboratory.

This report covers only the seismic measurements made by the U. S. Geological Survey. The first objective of this report is to describe the field recording procedures and the data obtained by the U. S. Geological Survey from these events. The second objective is to describe the spectral analyses which have been made on the data and the relative seismic amplitudes which have been determined from these analyses.

FIELD PROCEDURES

U. S. Geological Survey seismic recording systems (Warrick et al, 1961) were used for these experiments. Each system records the signal from eight seismometers on both photographic paper and magnetic tape. Six of the seismometers register vertical ground motion and two register horizontal ground motion. The six vertical seismometers are placed at 500-meter intervals and the two horizontal seismometers are located at one of the vertical seismometer positions near the center of the spread.

Individual seismometer locations are presented in Figures 2 through 9 with one complete spread shown in each figure. The Poplarville site (Figure 4) was occupied by two recording systems. The Poplarville, Picayune, and Raleigh locations used in October, 1964 to record the Salmon event, were duplicated as closely as possible for the Sterling event. Between the Sterling HE shot on November 17 and the Sterling nuclear event on December 3, the seismometers were left in place to insure duplication of recording

position for these two events. Seismometers were buried at a depth of from 6 to 12 inches, firmly placed and covered.

SYSTEM RESPONSE

The Electrotech EV-17 seismometer used in this experiment has a resonant frequency of one cycle per second (cps) and an approximately flat response to ground velocity from 1 cps to above 30 cps. The recording instruments have an approximately flat response from 1 cps to an upper limit imposed by the high-cut filter which is selected. For this experiment a filter with a cutoff at 37 cps was selected. The response of the system to ground displacement (Figure 10) is linear between 1 and 30 cps, and if converted to velocity, this portion of the response would be flat. The seismic recording systems were individually calibrated for this experiment and found to be closely matched in the range from 1 to 30 cps. Small differences in the recording systems do exist below 1 cps.

SEISMOGRAMS RECORDED

Playbacks were made from the 21 tape recordings (Figures 11-18) with a playback filter of out-37 cps (low-cut filters out; high-cut filters 37). The 10-cps sinusoidal signal appearing at the beginning of each trace is a calibration signal applied at the input to the recording unit and is used to calibrate the recording and playback electronics.

The Sterling nuclear and the Sterling HE events were recorded at the maximum sensitivity permitted by the seismic background noise with the exception that channels two and five of the three stations nearest to the shot point were recorded with an additional 6 to 12 db of attenuation for the Sterling nuclear event. The Salmon event was recorded at much higher attenuation levels based on our pre-shot estimates of Salmon amplitudes. It is important to note that the noise on the seismograms and magnetic tapes from the Sterling nuclear and Sterling HE events is predominantly seismic noise, while the noise on the Salmon event has been introduced primarily by the recording system.

SPECTRAL ANALYSIS

The analysis plan was based on the assumption that the motion surrounding the three seismic sources could be described as the product of a function of time and a function of the space coordinates where the function of the space coordinates is identical for all three sources. If this assumption is true the variation between the seismic signals recorded at the same point for the different shots will reflect only the time variation in the source function, and the ratio of the source spectra for any two shots can be obtained by taking the ratio of identical portions of the seismic signal recorded for the two shots.

We, therefore, chose to analyze a constant 11-second interval on each seismogram without regard to the phases that were included within this interval. The 11-second interval for each seismogram began one second before the first identifiable seismic energy appeared on the seismogram.

An analog-to-digital converter system was used to prepare the data for an IBM 7090 computer. The data was digitized at 0.01-second intervals. A digitization interval of 0.005 seconds was used for comparison on some of the data with no resulting change in the spectral amplitudes up to 40 cps. Four seconds of the 10-cps sinusoidal calibration signal was also digitized and used to calibrate the seismic signals in the computer.

The amplitude spectra have been computed from the expression, $\left| \int_{1}^{11} v(t) e^{-iwt} \, dt \right|$ where t=0 is the time of the first identifiable energy on the seismogram and v(t) represents the data on a seismic trace after the amplitudes have been normalized by the calibration signal. The integral was evaluated using the Filon quadrature (Filon, 1928).

The computer program which was written for these computations was tested with an exponentially decaying sine function and had an accuracy better than 0.05% for frequencies up to 50 cps.

The resulting amplitude spectra for all individual seismic traces are shown in Figures 19-30. The amplitude scale in microvolts

is based on the 10-cps calibration signal and does not take into account the variation of system response with frequency. The amplitude spectra for Sterling have been placed next to the corresponding spectra for Salmon (Figures 19-21) and for Sterling HE (Figures 22-30) to make their comparison easier. Numerical values of the spectra were punched on computer input cards, which were in turn used to compute ratios of amplitude spectra. The ratios are shown in column 3 of Figures 19-30.

Ratios were not computed when a seismic trace was unreliable for any reason. For example, note the Keno recordings (Figure 11 and 22) where the attenuation settings are too low and the magnetic tapes were clipped. On a number of recordings individual traces were excluded.

Noise spectra were made in the same manner for the Salmon and Sterling recordings at the Poplarville, Picayune, and Raleigh sites (Figures 31-32). An 11-second interval of background noise, just before the signal arrival, was used for this analysis so that the resulting spectra can be compared with those in the preceding figures to estimate the effect of noise on the spectra of the signals.

The amplitude ratios from individual traces were averaged to form an average spectral ratio for each recording site. Thus there are three average plots for the Salmon to Sterling nuclear (Figures 33-35) and eight average plots for Sterling HE to Sterling

nuclear (Figure 36). Finally, the ratios from all usable individual traces were averaged to form a single plot for the Salmon to Sterling nuclear (Figure 37) and one for the Sterling HE to Sterling nuclear (Figure 38).

CONCLUSIONS

The seismic noise and the system noise limit the accuracy of the spectra and the spectral ratios, particularly at the higher and lower frequencies. Based on examination of the noise spectra and our knowledge of the system response, we have estimated that the spectra give a valid indication of source properties between 0.8 and 25 cps. At frequencies higher or lower than these values the spectral plots may be seriously in error. The zones of questionable reliability are indicated in Figures 37 and 38 by cross hatching.

An examination of all the spectral plots reveals a marked difference in the detailed structure of the spectra of individual seismic traces, but, in general, there is considerable similiarity in the gross shape of the spectra. This is particularly true of the spectral ratios, which appear to be similar at all recording locations.

This similiarity tends to confirm our original assumption that the source function could be expressed as a product of two functions separating the variation in time from the variation in space. Insofar as this is true, it justifies our averaging procedure and suggests

that these spectral ratios can be used to estimate the decoupling effect at greater distances.

DECOUPLING

An estimate of the decoupling of the Sterling nuclear event is beyond the scope of this report. Such an estimate requires precise determination of the yields of the three events, and a precise scaling law that will predict the seismic signal from a tamped nuclear shot of the same size as the decoupled Sterling nuclear shot. Further, the estimate of decoupling from this experiment should be based on an examination of all the available data including the surface seismic data from the U. S. Coast and Geodetic Survey and the Air Force Technical Applications Center and the near shot subsurface data recorded by Sandia Corporation.

However, certain qualitative conclusions about decoupling can be drawn from these data. In the frequency range which predominates in teleseismic signals, between 1 and 5 cps, the Sterling nuclear event produced about the same seismic amplitudes as the Sterling HE event, but at higher frequencies the Sterling nuclear event produced more seismic energy than the Sterling HE event.

In the frequency range between 1 and 5 cps, the Salmon nuclear event produced seismic amplitudes about 1000 times as large as the decoupled Sterling nuclear, but at frequencies between 10 and 25 cps, the seismic signals from Salmon were less than 200 times as large as the seismic signals from the Sterling nuclear.

Table 1.--Station Locations

Station	HE Sterling Distance (km)	Salmon and Sterling Distance (km)	Latitude	Longitude
Keno E	13.7	13.5	31°13.86'	89°40.00'
Keno W	15.5	15.3	31°14.04'	89°41.39'
Rouse W	15.8	16.2	31° 0.56'	89°38.94'
Rouse E	17.3	17.7	30°59.49'	89°37.86'
Poplarville (Hotel) E	26.3	26.6	30°54.14'	89°35.11'
Poplarville (Papa) E	26.3	26.6	31°54.14'	89°35.11'
Columbia E	27.6	27.7	30° 8.23'	89°51.60'
Poplarville (Hotel) W	28.4	20.7	30°53.00'	89°35.18'
Poplarville (Papa) W	28.4	28.7	30°53.00'	89°35.18'
Columbia W	30.1	30.1	31° 7.98'	89°53.15'
Sumrall W	31.1	30.8	31°25.15'	89°35.00'
Sumrall E	33.1	32.8	31°26.26'	89°34.86'

Table 1.--Station Locations

Station	HE Sterling Distance (km)	Salmon and Sterling Distance (km)	Latitude	Longitude
Camp Shelby W	39.0	38.9	31° 8.84'	89° 9.75'
Camp Shelby E	40.9	40.8	31° 8.88'	89° 8.50'
Picayune E	67.0	67.4	30°32.10'	89°32.37'
Picayune W	69.5	69.8	30°30.77'	89°32.47'
Raleigh W	109.8	109.4	32° 7.70'	89°36.99'
Raleigh E	112.2	111.9	32° 9.02'	89°36.80'

REFERENCES

Filon, L. N. G., Proc. Roy. Soc., Edinburgh, (A) 49, 38, 1928.

Warrick, R. E., D. B. Hoover, W. H. Jackson, L. C. Pakiser, and J. C. Roller, 1961, The Specification and Testing of a Seismic-refraction System for Crustal Studies; Geophysics, v. 26, no. 6, p. 820-824.

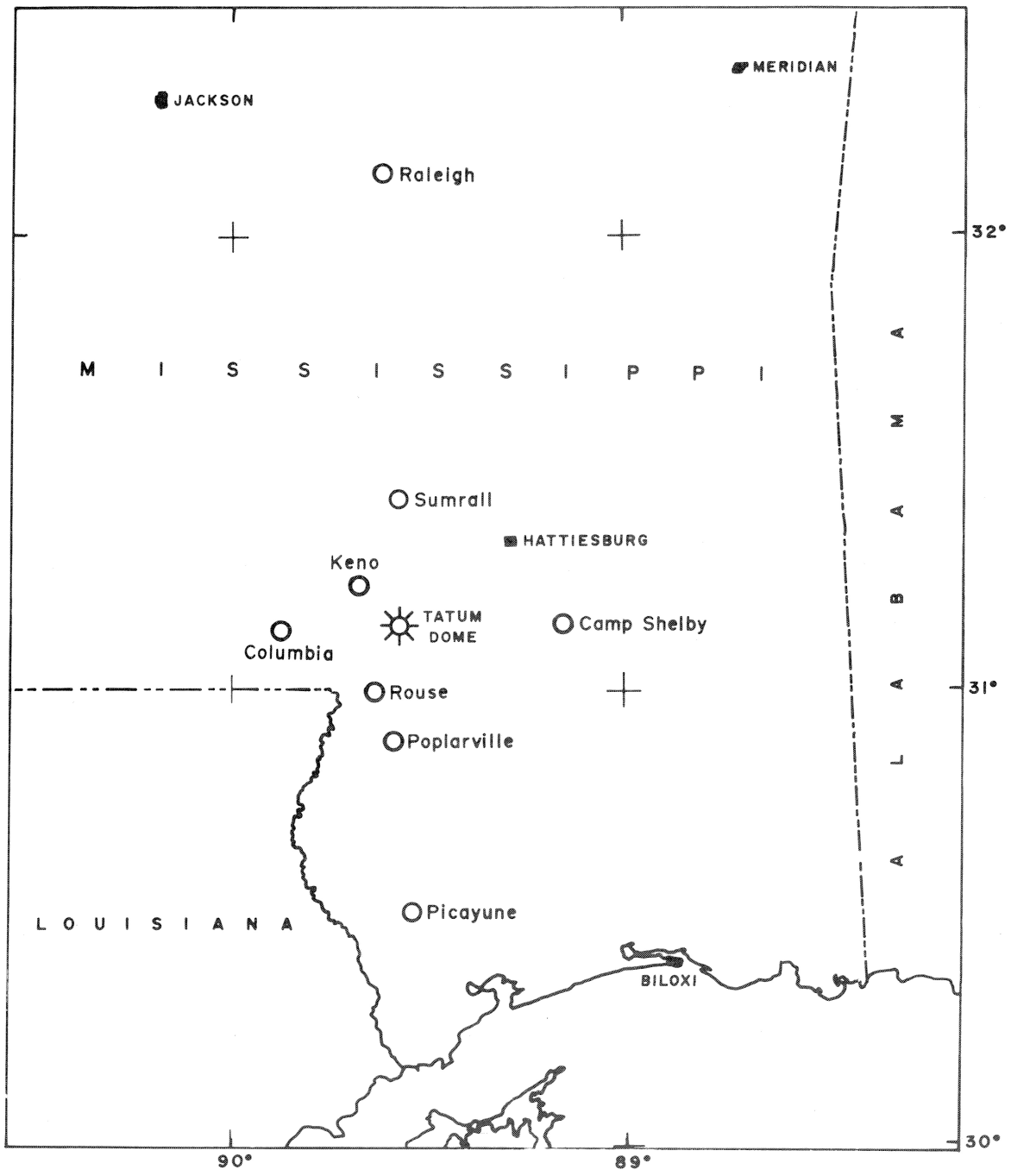

Figure 1.--Location map

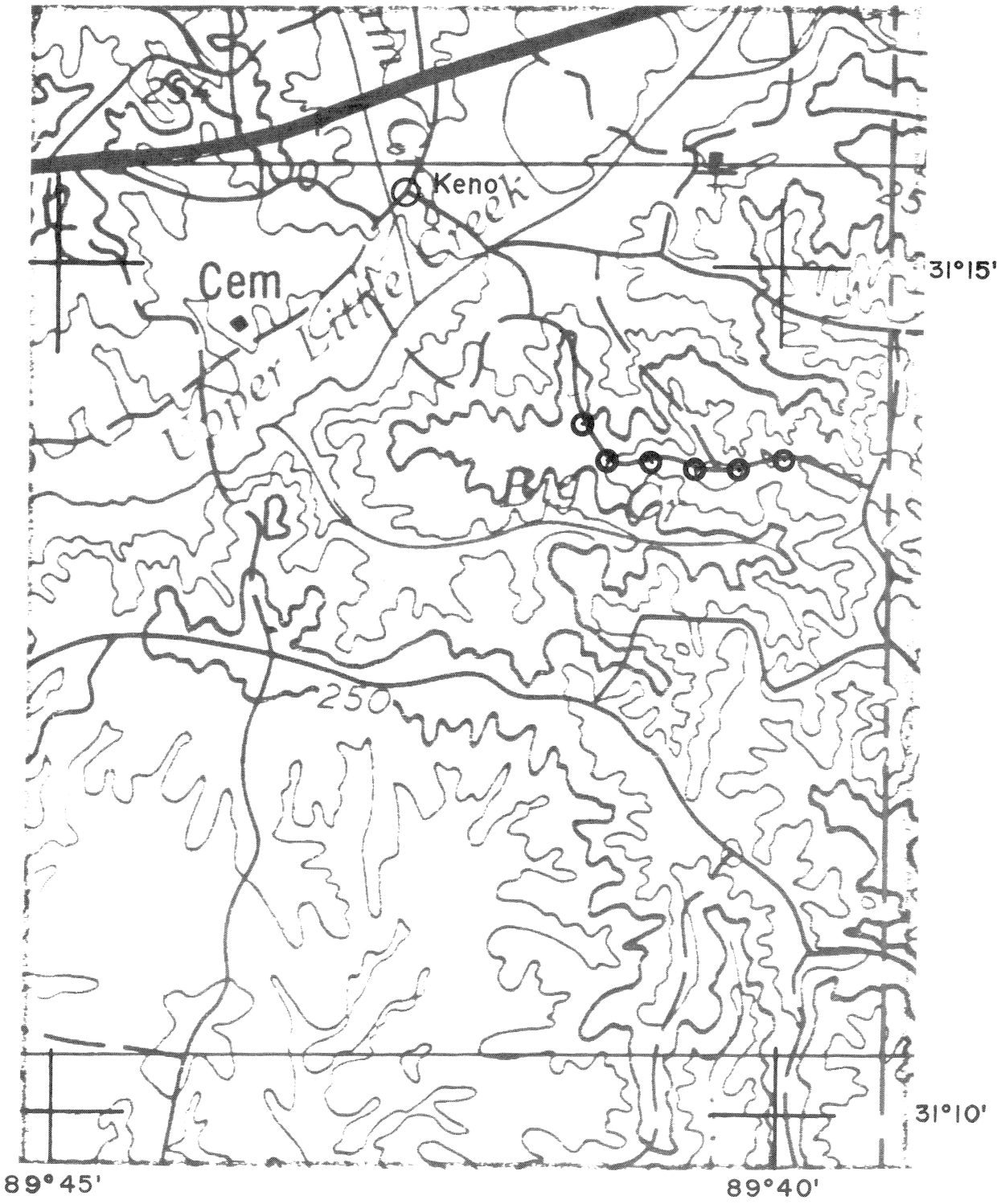

Figure 2.--Keno recording site

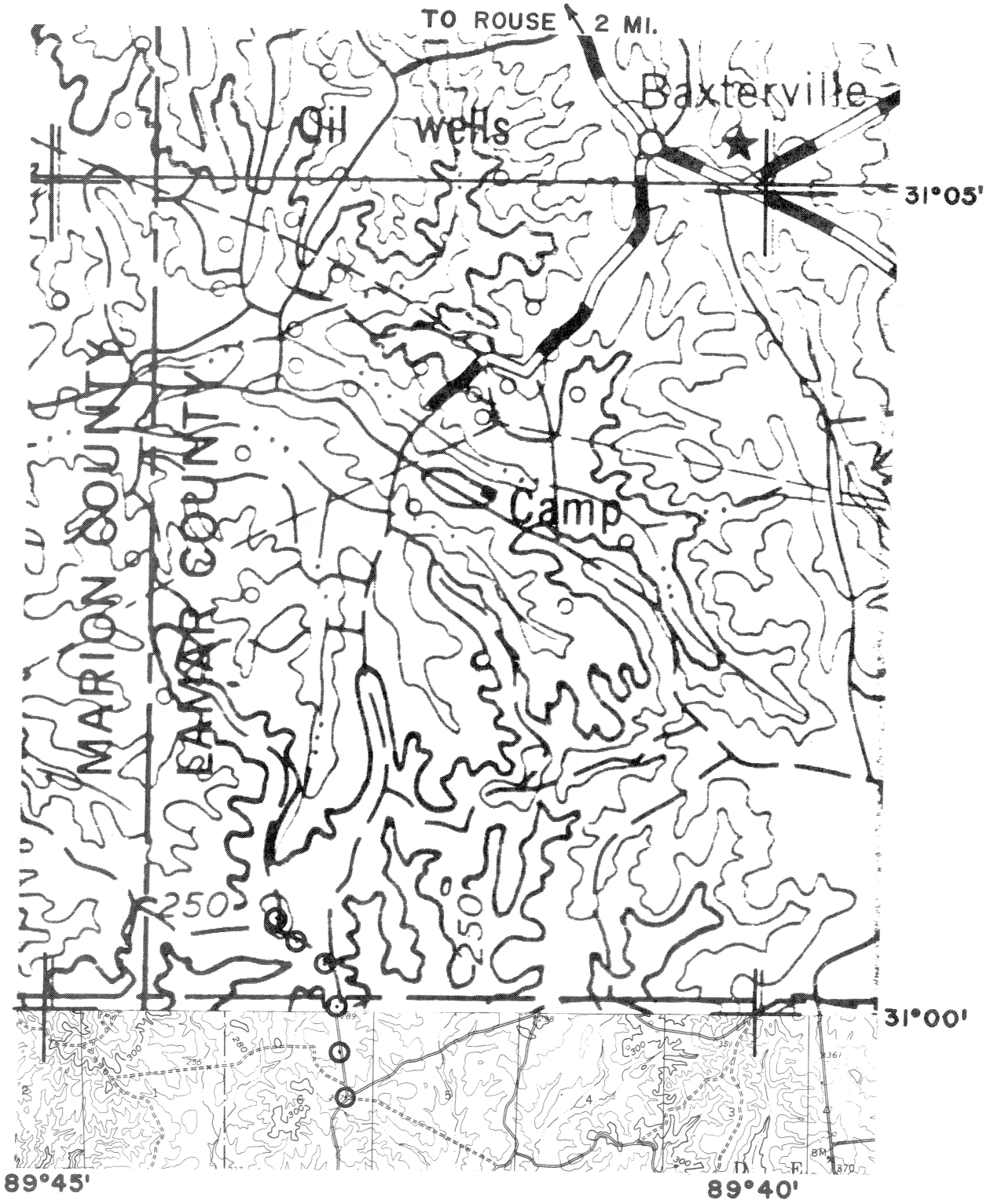

Figure 3.--Rouse recording site

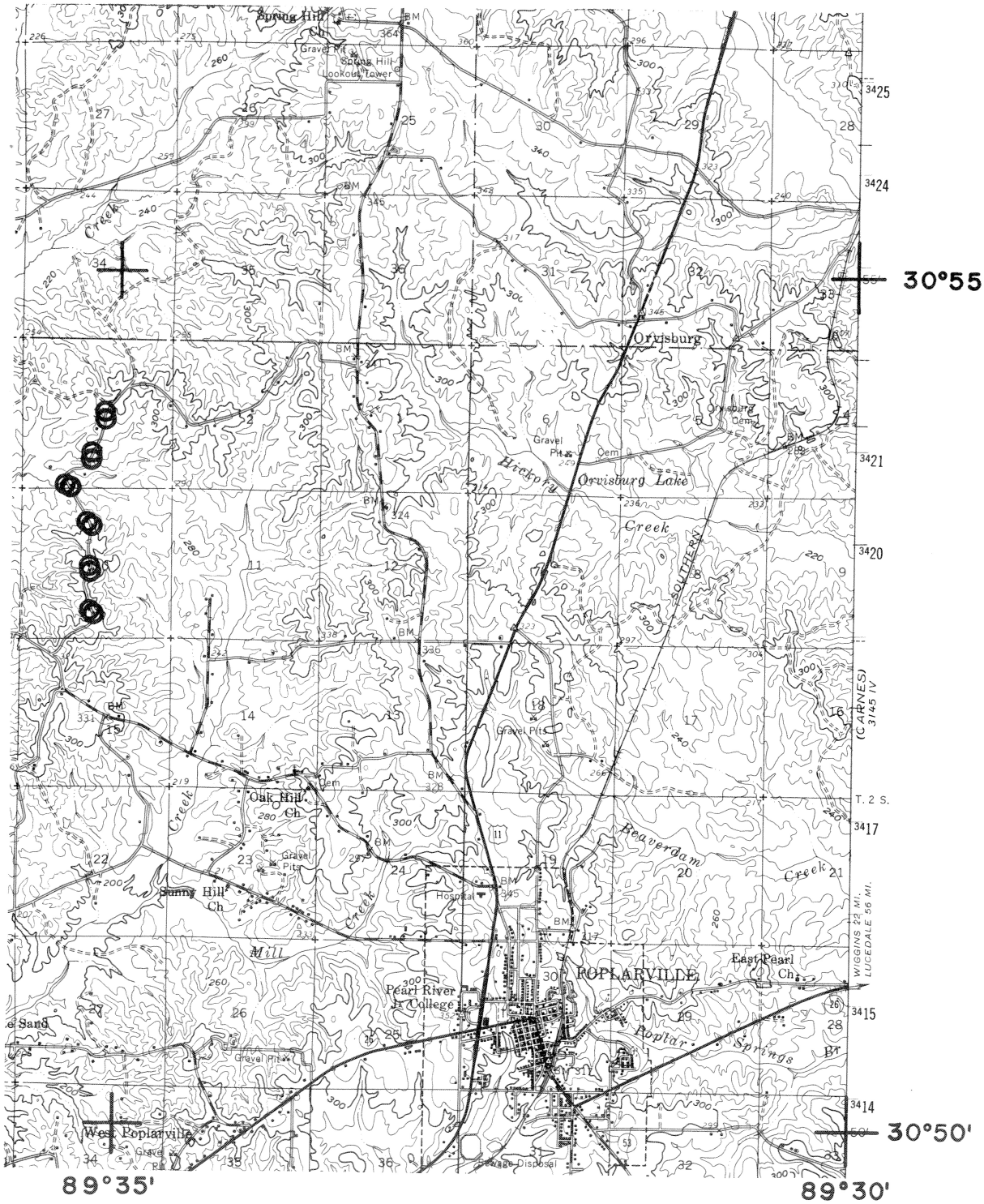

Figure 4.--Poplarville recording site

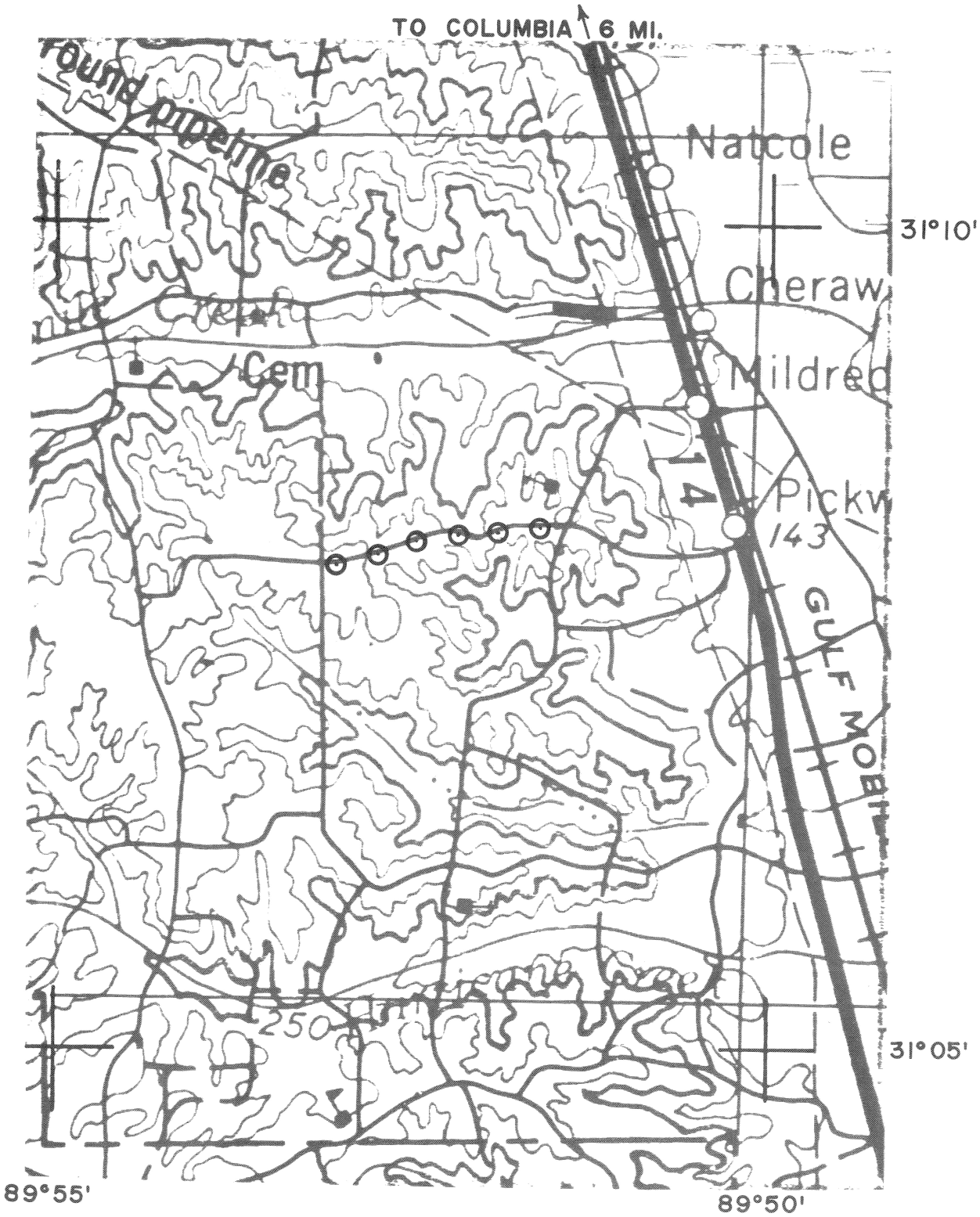

Figure 5.--Columbia recording site

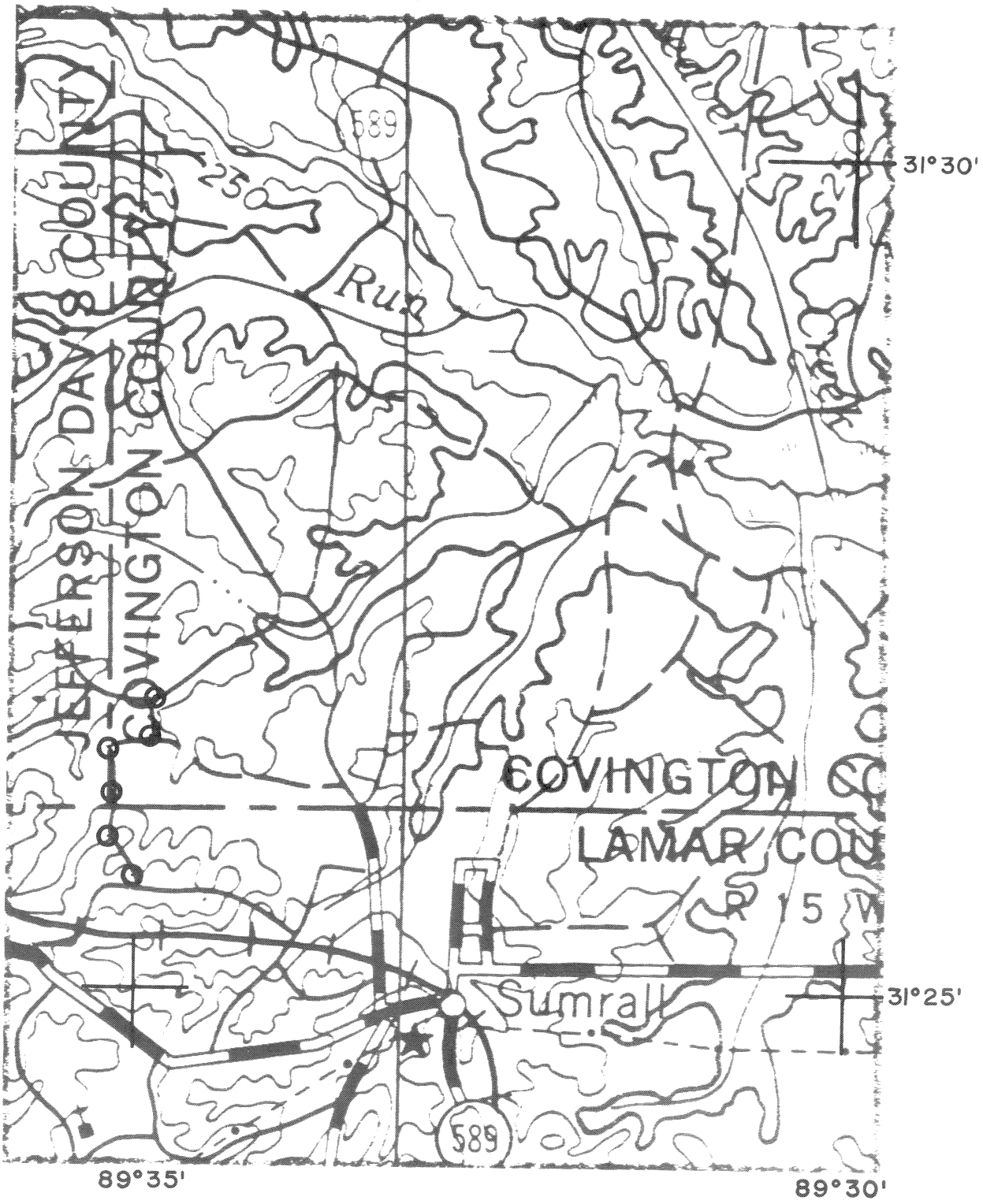

Figure 6.--Sumrall recording site

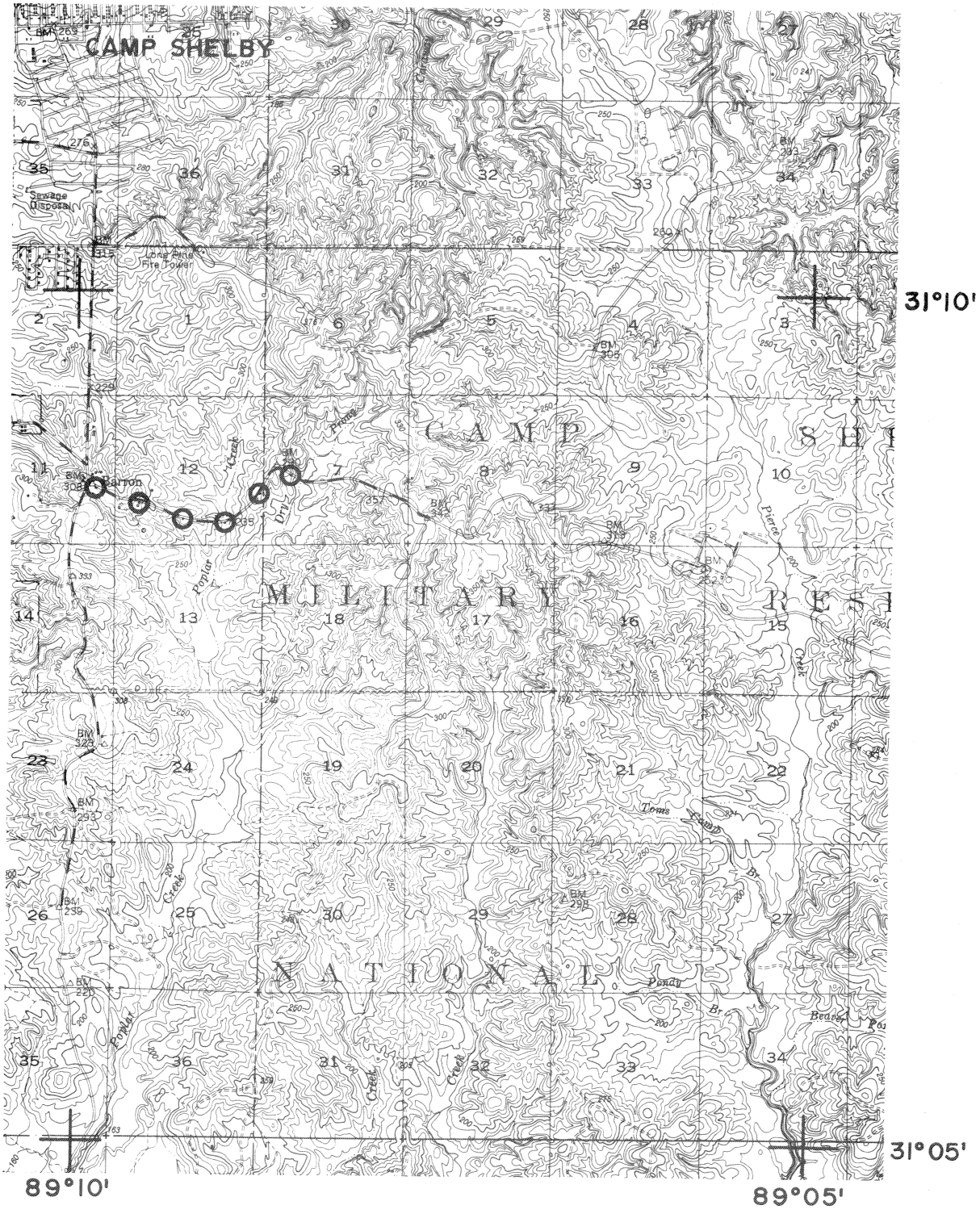

Figure 7.--Camp Shelby recording site

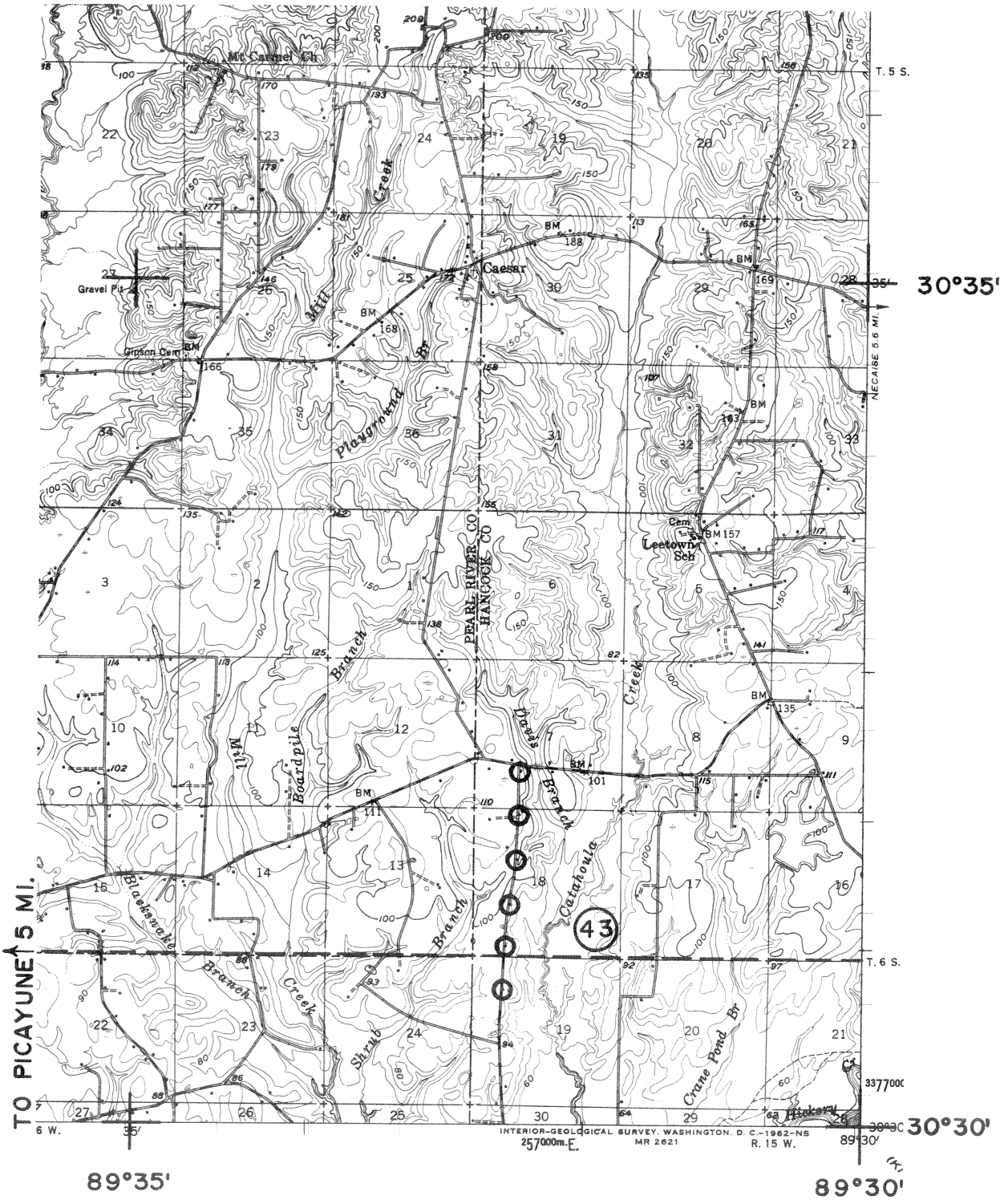

Figure 8.--Picayune recording site

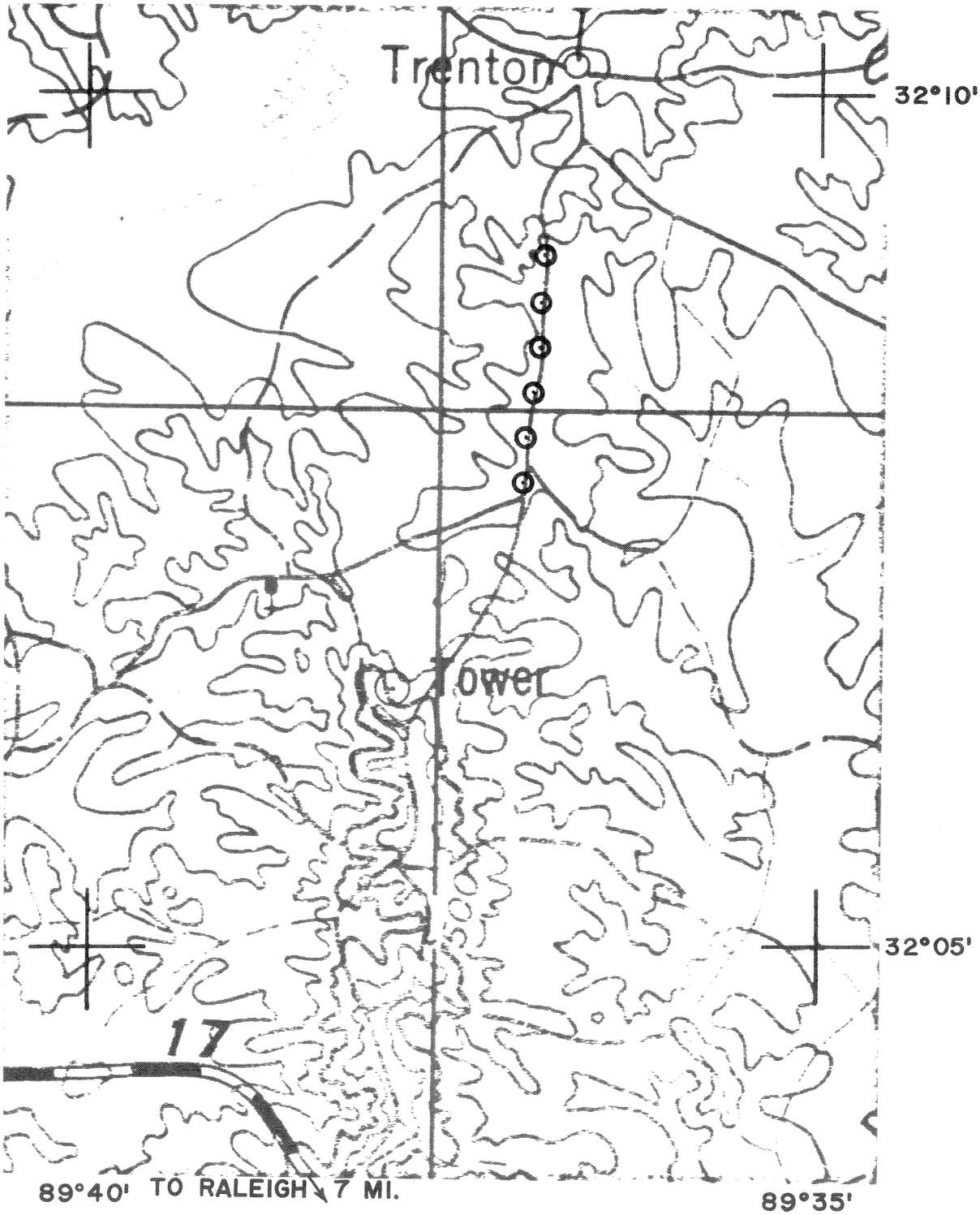

Figure 9.--Raleigh recording site

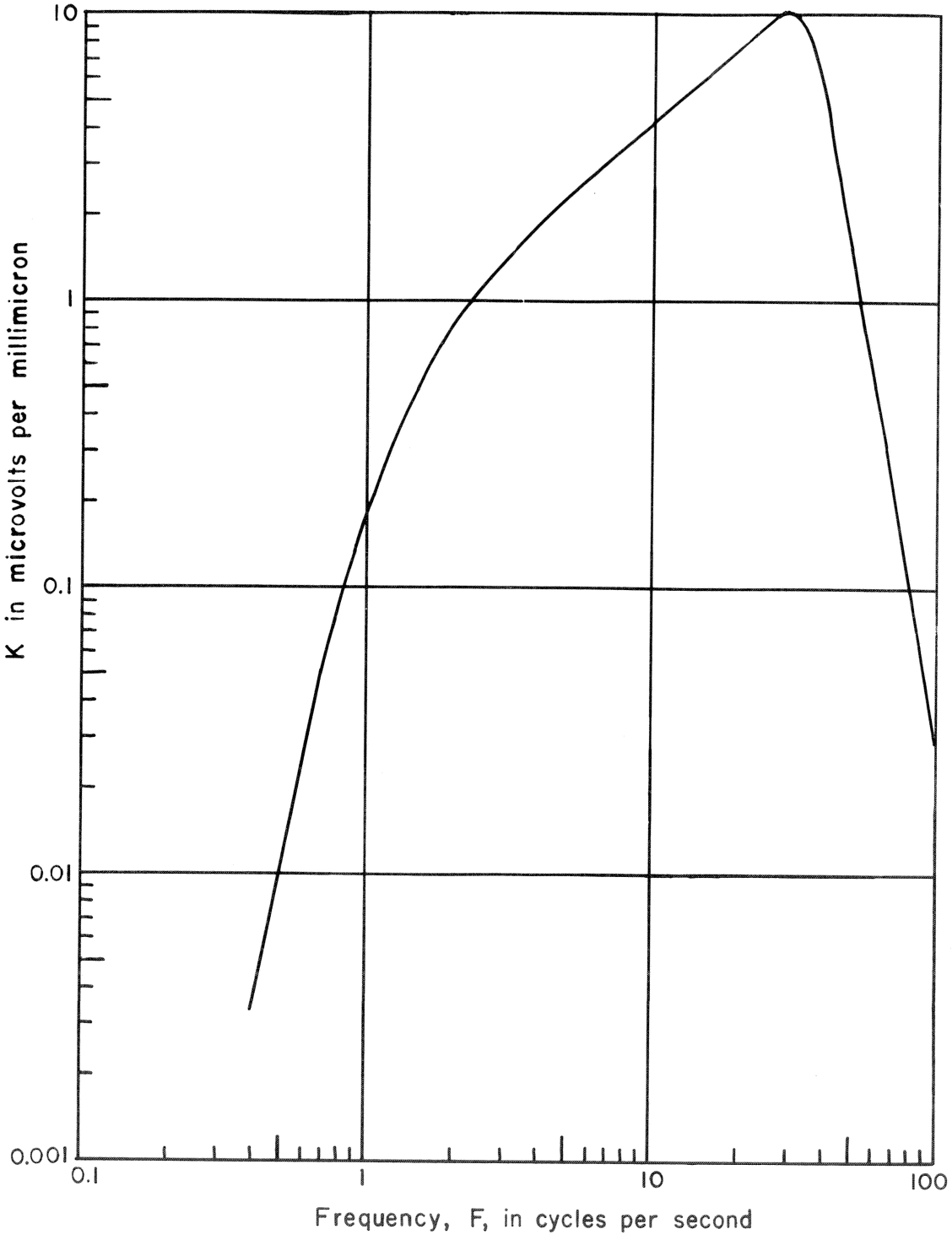
10
1
0.1
0.01
0.001
K in microvolts per millimicron
0.1
1
10
100
Frequency, F, in cycles per second

Figure 10

Use of System-Calibration Plot

$$A = \frac{SV}{CK} \quad \text{where,}$$

A is amplitude of ground displacement in millimicrons (10^{-9} meters);

S is the peak-to-peak amplitude of a selected phase on a seismogram in any convenient units;

V is the calibration voltage in microvolts;

C is the peak-to-peak amplitude of the calibration signal in the same units chosen for measurement of S; and

K is a constant, in microvolts/millimicron, obtained from the enclosed system-calibration plot. The abscissa, F, on this plot is the frequency in cps of the phase for which S was measured.

The amplitude of ground displacement, A, determined by application of this equation is the displacement relative to the rest position of the ground.

If you want the velocity of ground displacement, v_p, in millimicrons/second use:

$$v_p = 2\pi F A$$

Similarly, acceleration, a_p, in millimicrons/second/second is given by:

$$a_p = 4\pi^2 F^2 A$$

Figure 10b

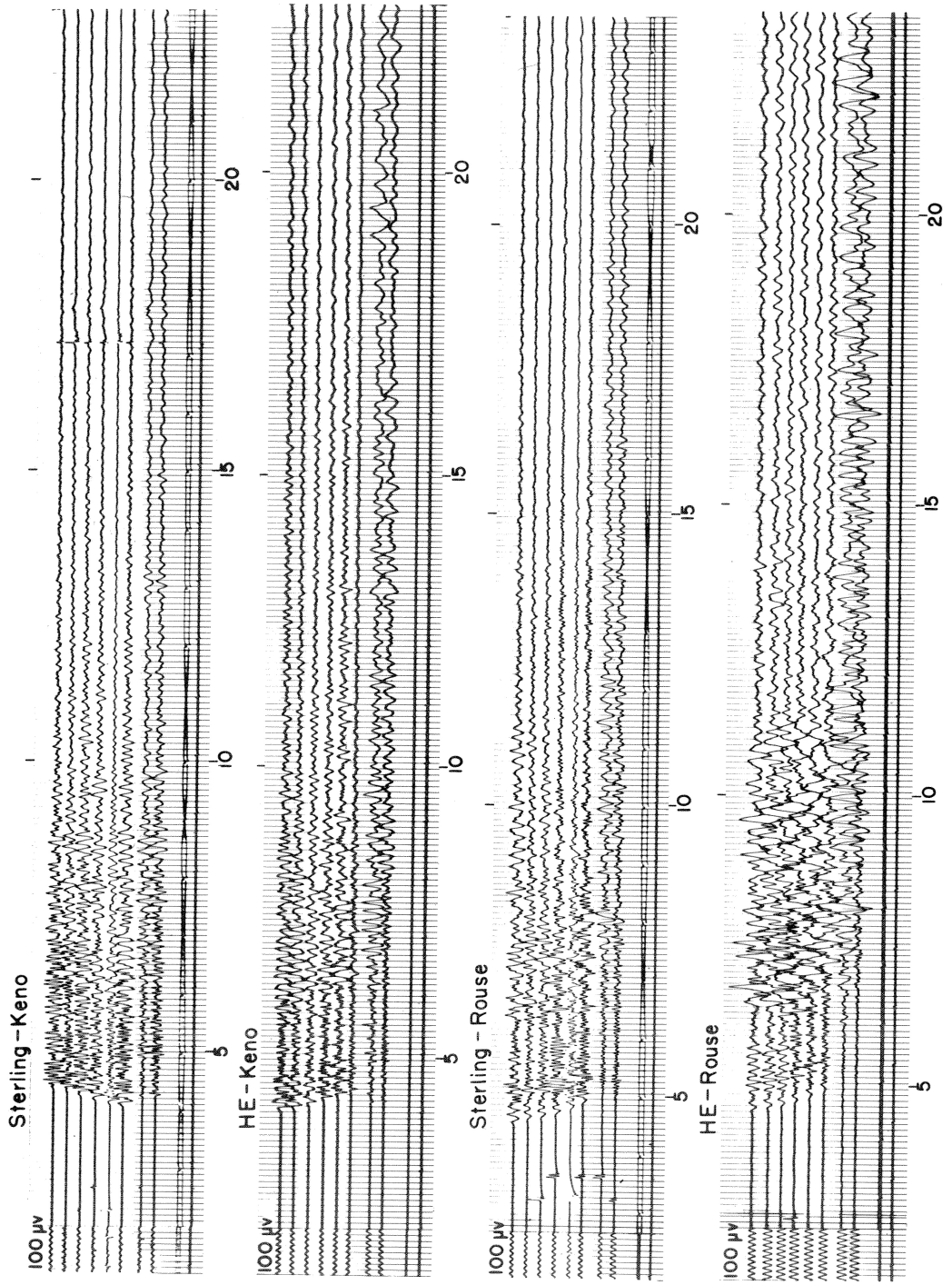
Sterling-Keno
HE-Keno
Sterling-Rouse
HE-Rouse
100 µv
5
10
15
20

Figure 11

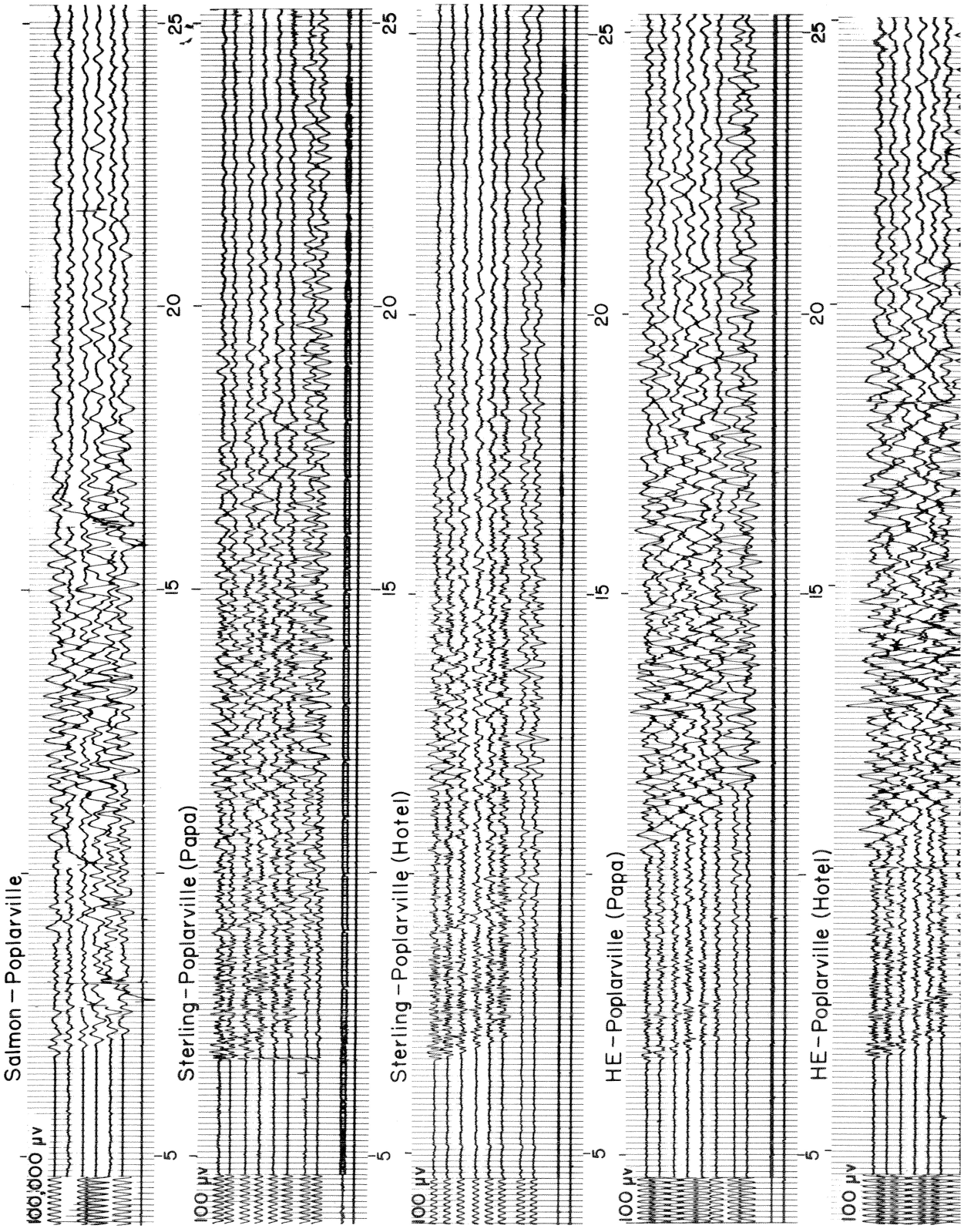
Salmon – Poplarville
100,000 µv
Sterling – Poplarville (Papa)
100 µv
Sterling – Poplarville (Hotel)
100 µv
HE – Poplarville (Papa)
100 µv
HE – Poplarville (Hotel)
100 µv
5
15
20
25

Figure 12

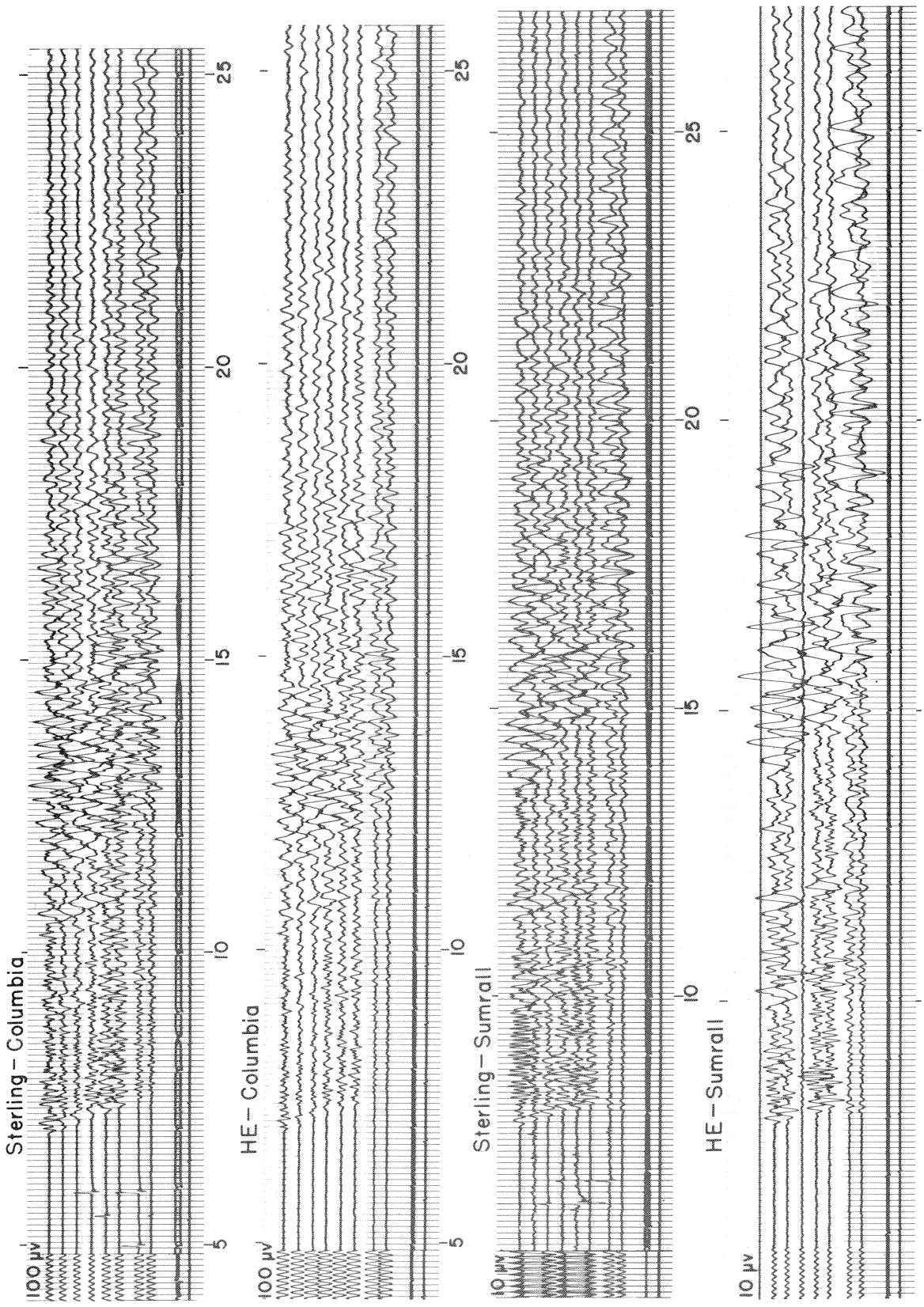
Sterling – Columbia
HE – Columbia
Sterling – Sumrall
HE – Sumrall
100 µv
100 µv
10 µv
10 µv
5
10
15
20
25

Figure 13

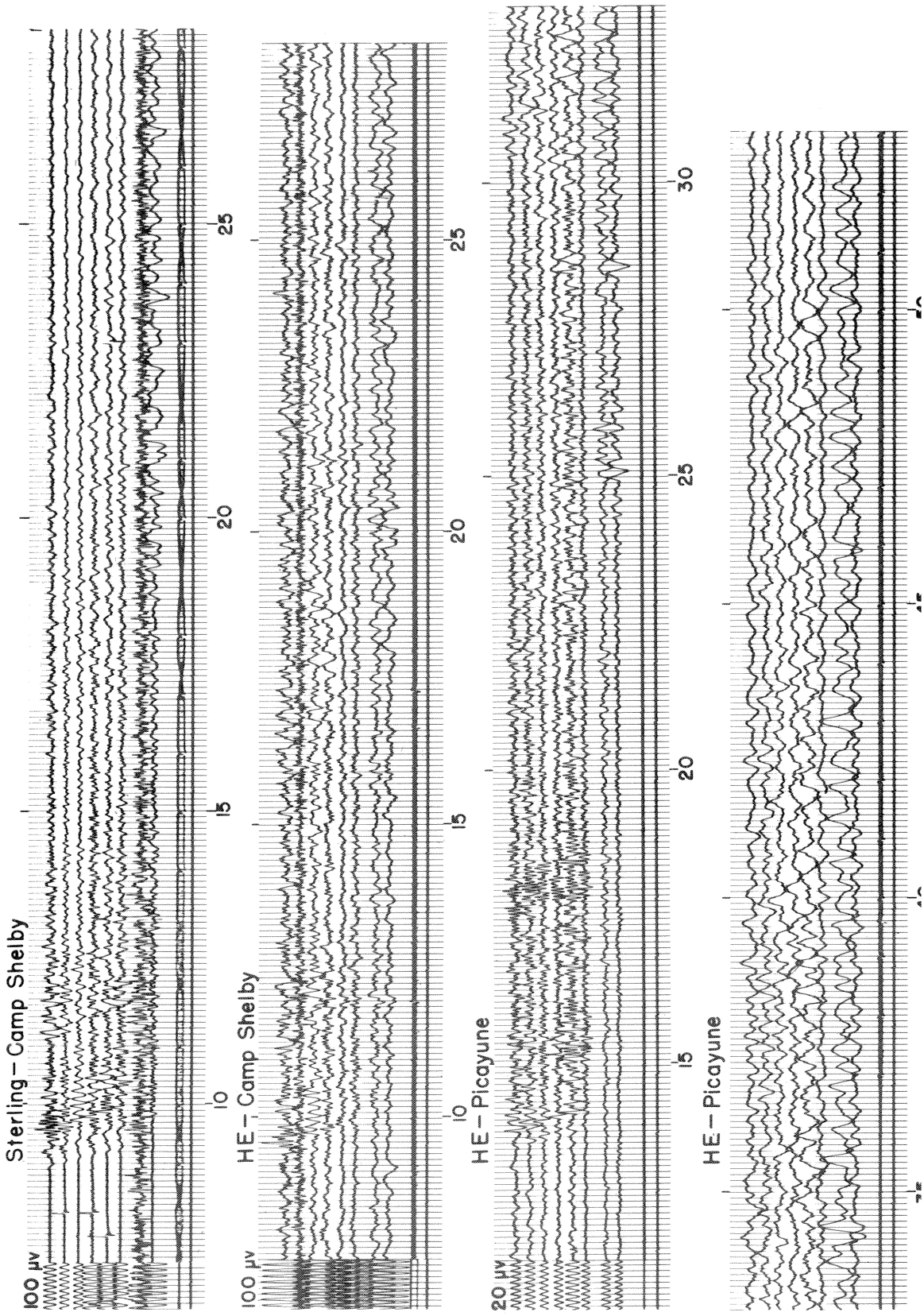
Sterling – Camp Shelby
100 μv
HE – Camp Shelby
100 μv
HE – Picayune
20 μv
HE – Picayune
10
15
20
25
30

Figure 14

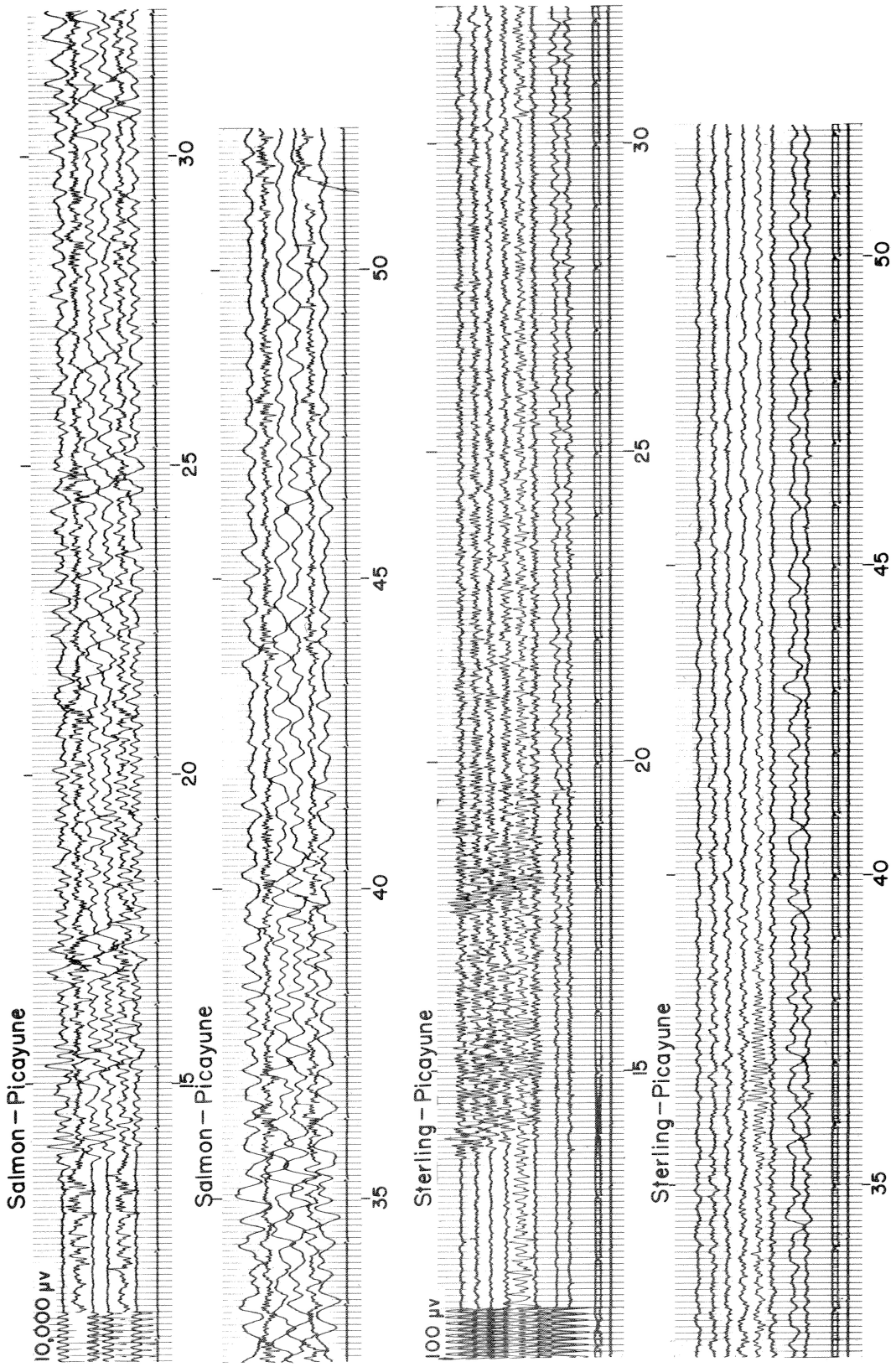
Salmon – Picayune
10,000 µv
Salmon – Picayune
Sterling – Picayune
100 µv
Sterling – Picayune
15
20
25
30
35
40
45
50

Figure 15

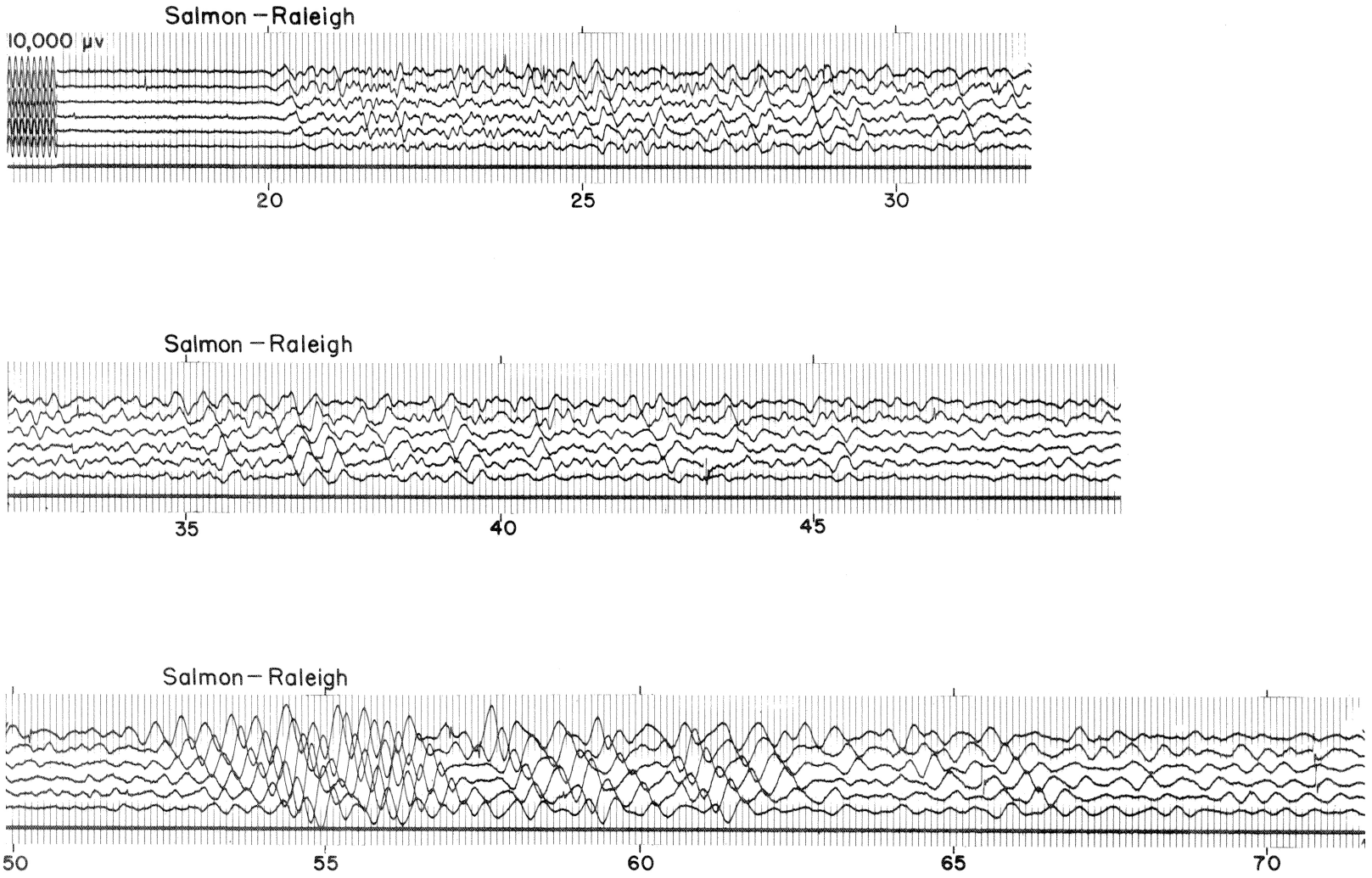
Salmon – Raleigh
10,000 µv
20
25
30
Salmon – Raleigh
35
40
45
Salmon – Raleigh
50
55
60
65
70

Figure 16

Sterling – Raleigh
10 μv
20
25
30
Sterling – Raleigh
35
40
45
50
Sterling – Raleigh
55
60
65
70

Figure 17

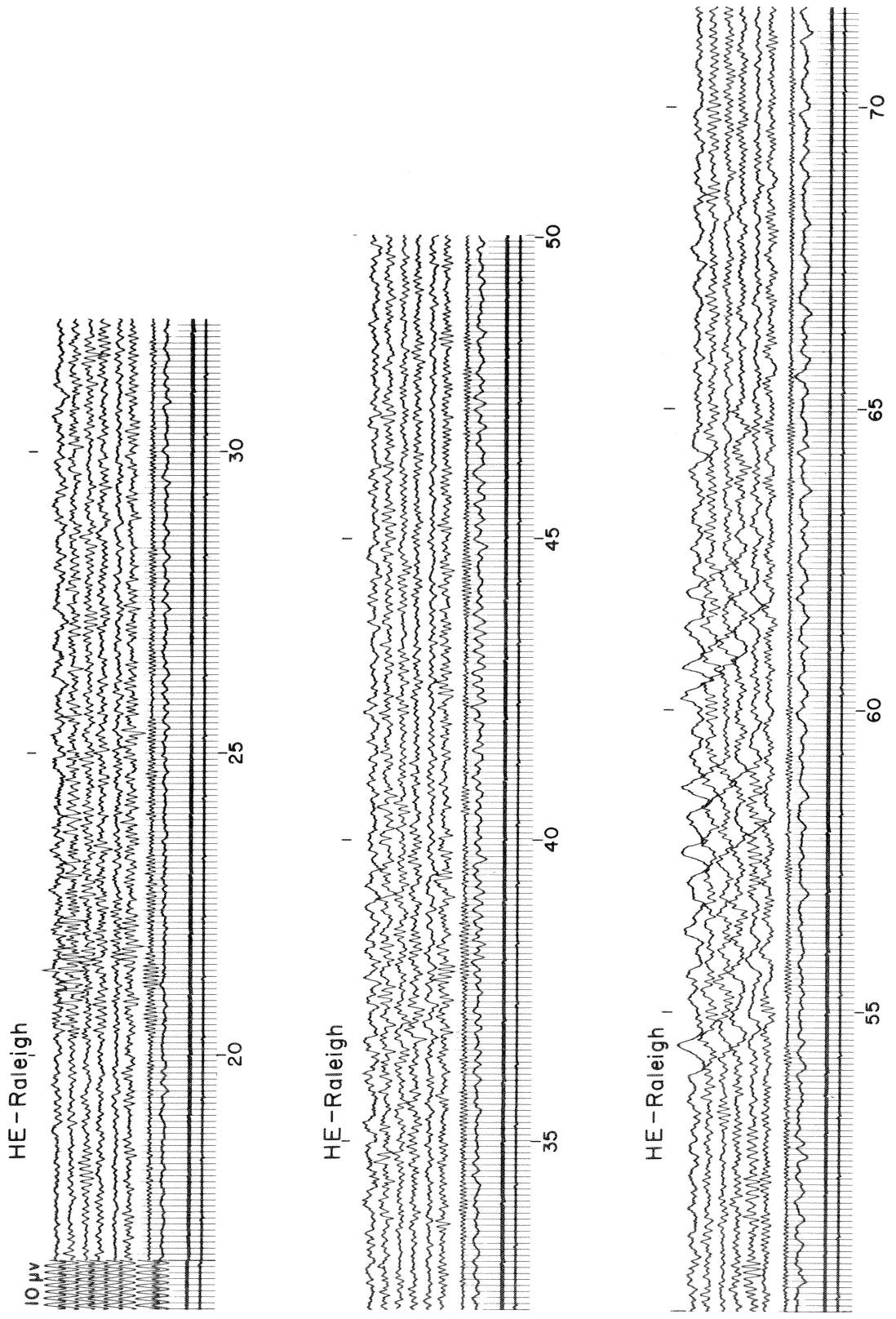
HE-Raleigh
10 μv
20
25
30
HE-Raleigh
35
40
45
50
HE-Raleigh
55
60
65
70

Figure 18

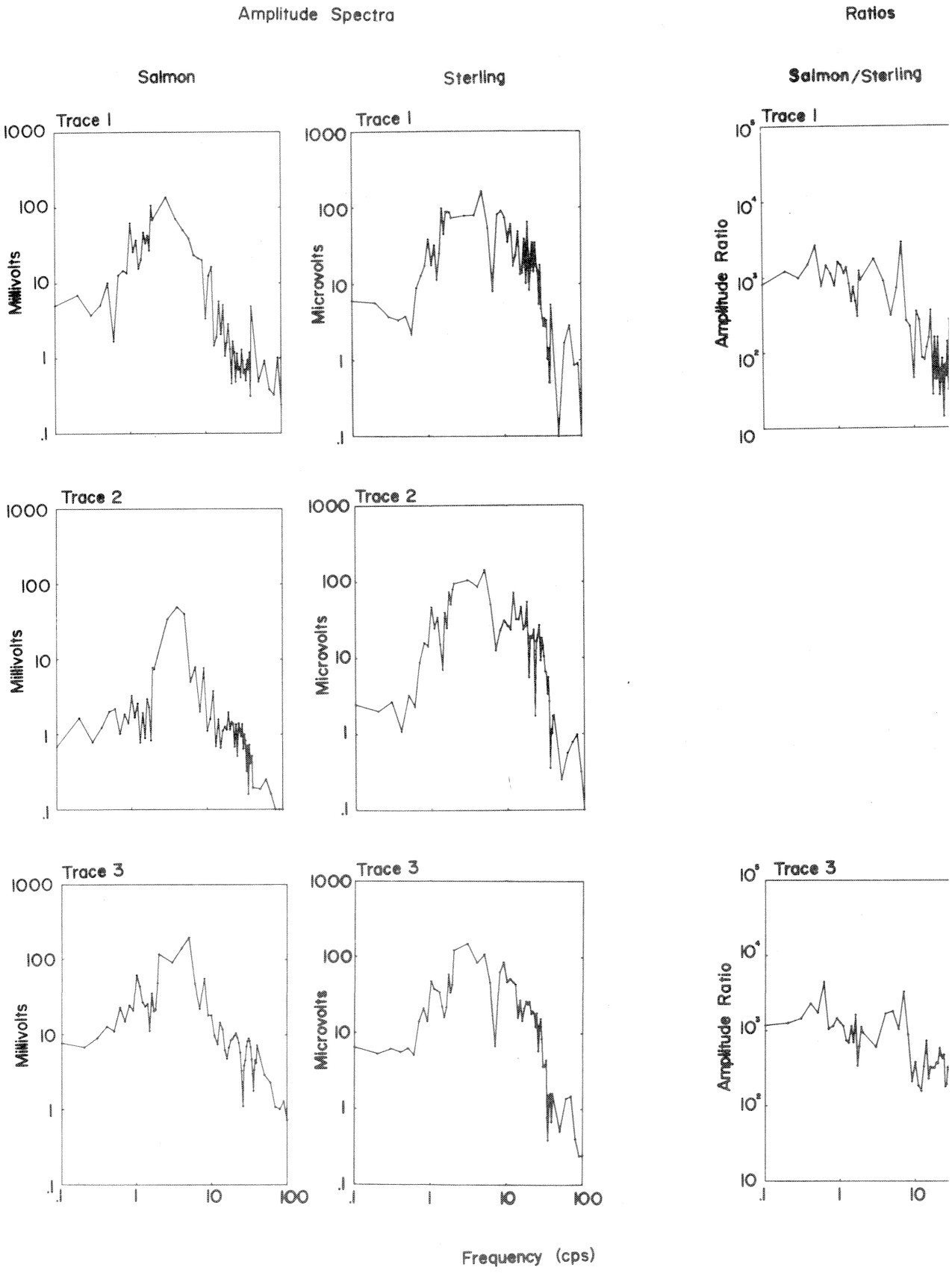

Figure 19a (Hotel)

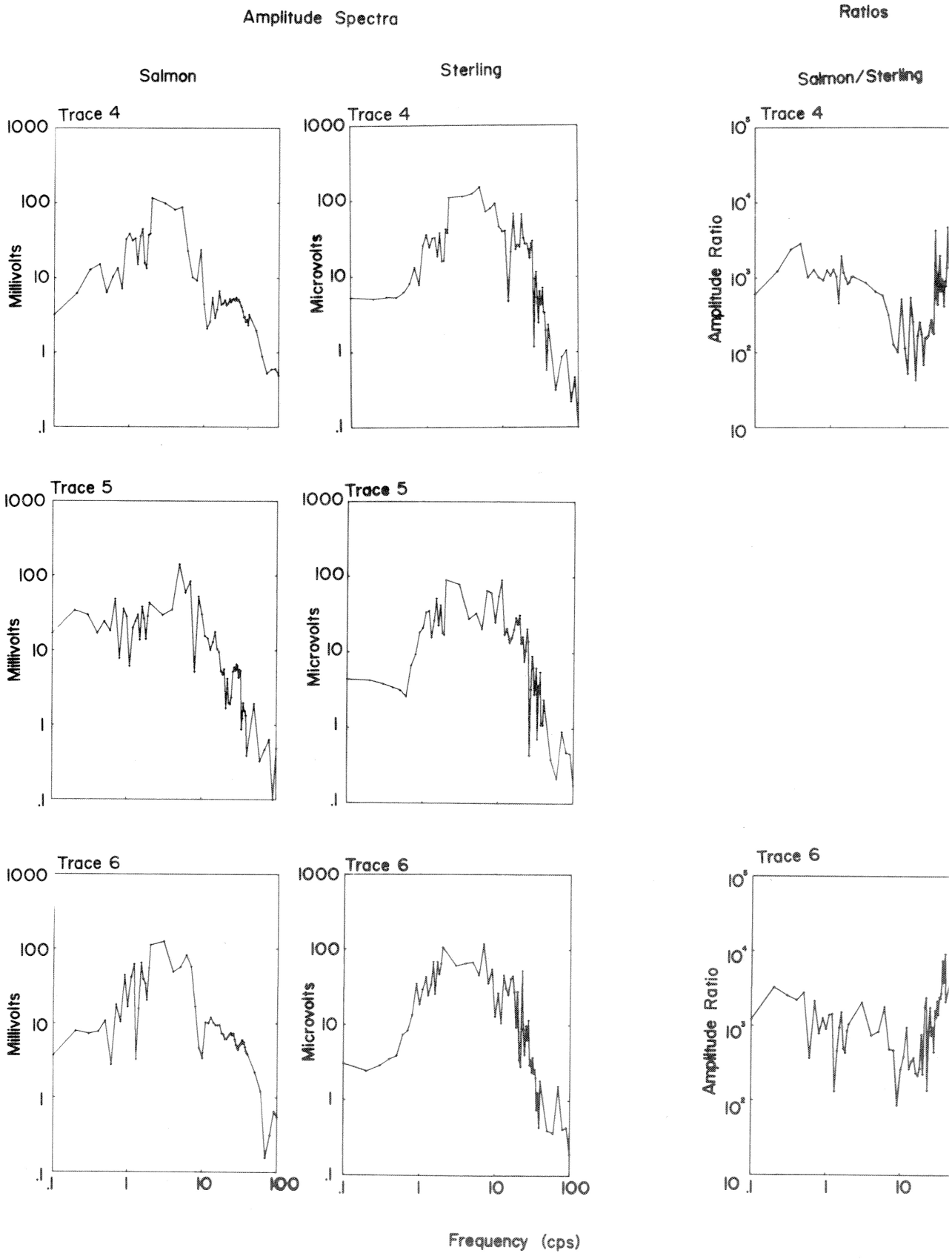

Figure 19b (Hotel)

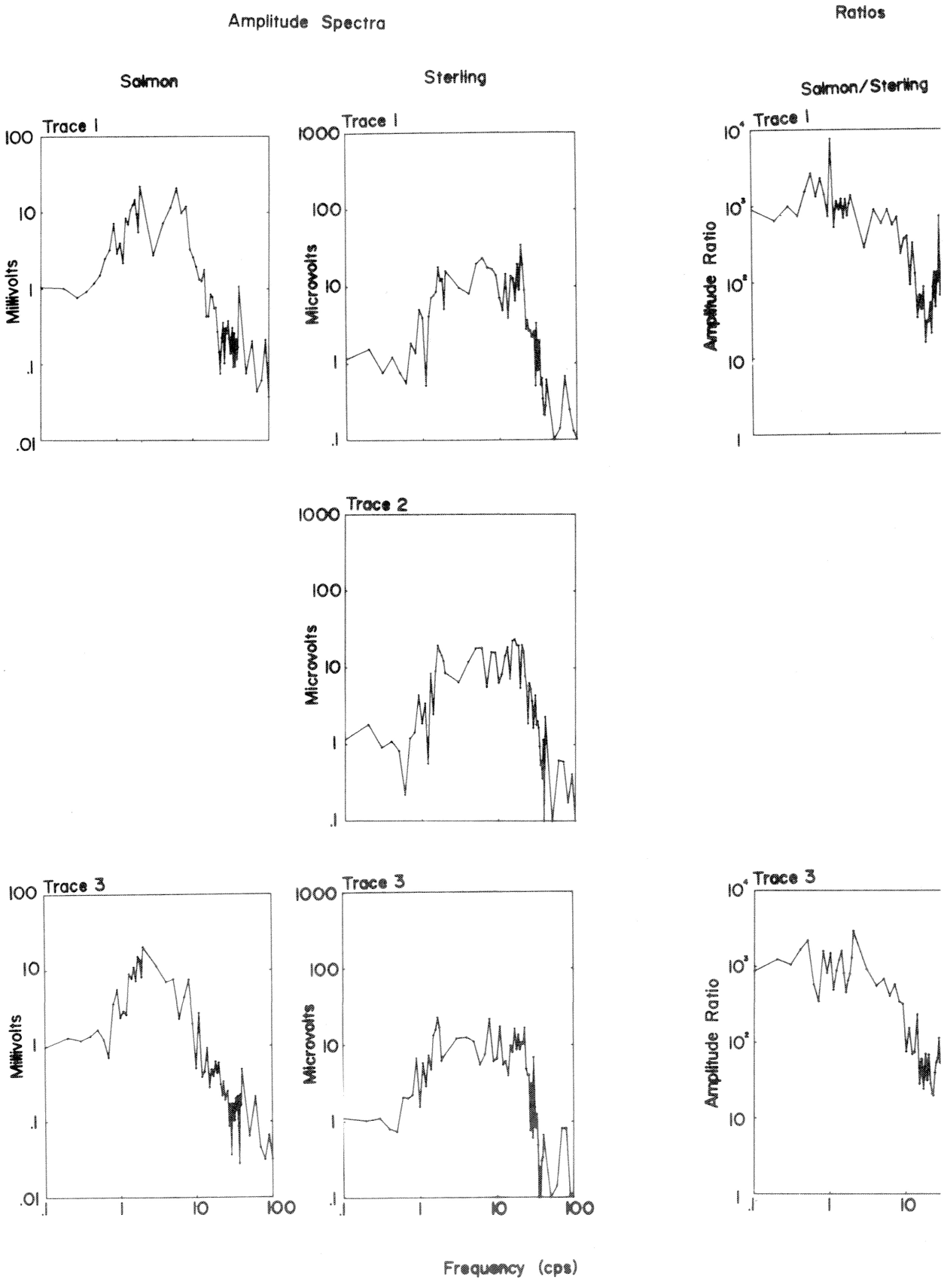
Amplitude Spectra
Ratios
Salmon
Sterling
Salmon/Sterling
Trace 1
Trace 2
Trace 3
Millivolts
Microvolts
Amplitude Ratio
100
10
1
.1
.01
1000
10^4
10^3
10^2
Frequency (cps)

Figure 20a

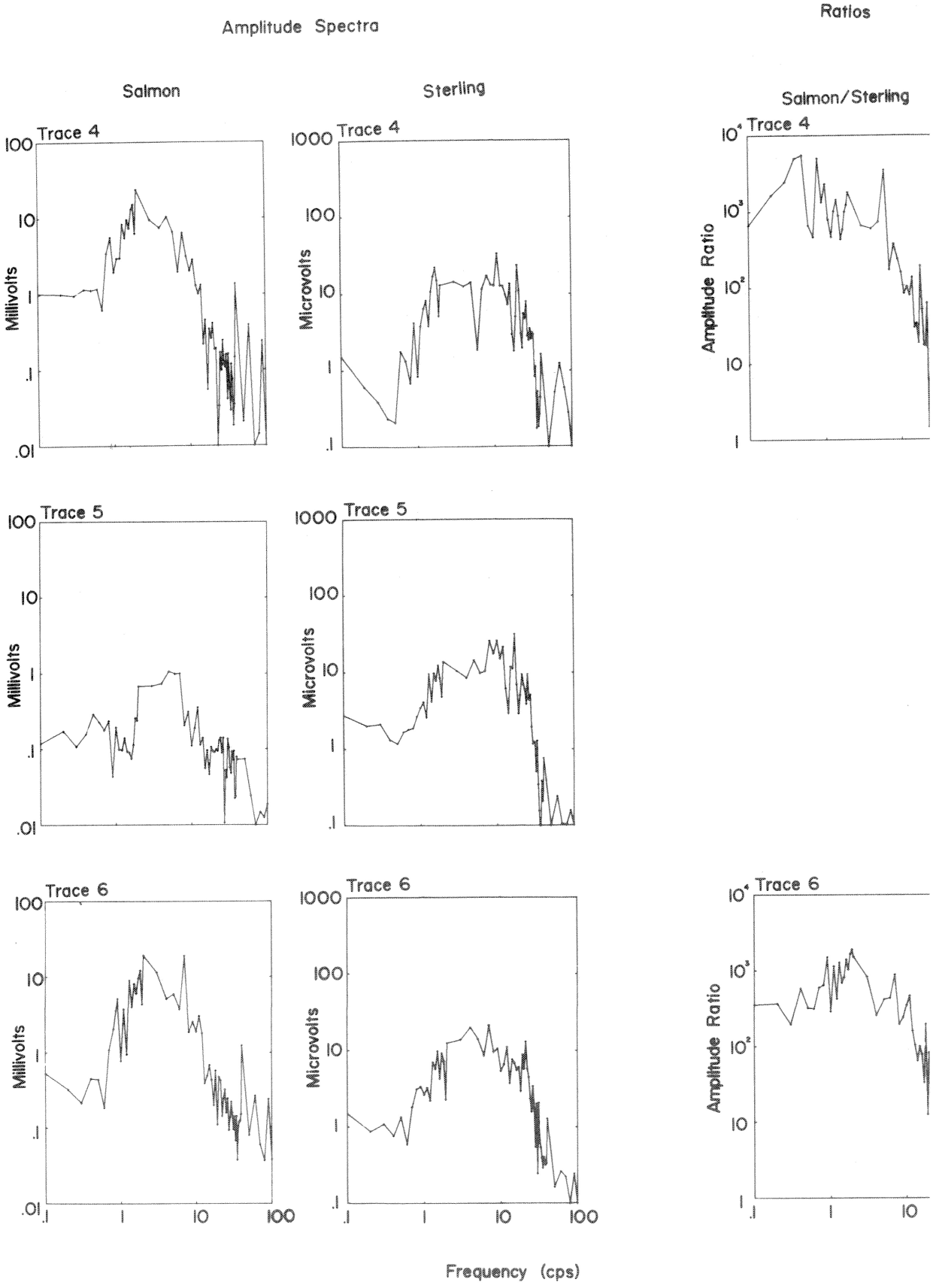
Amplitude Spectra
Ratios
Salmon
Sterling
Salmon/Sterling
Trace 4
Trace 5
Trace 6
Millivolts
Microvolts
Amplitude Ratio
Frequency (cps)

Figure 20b

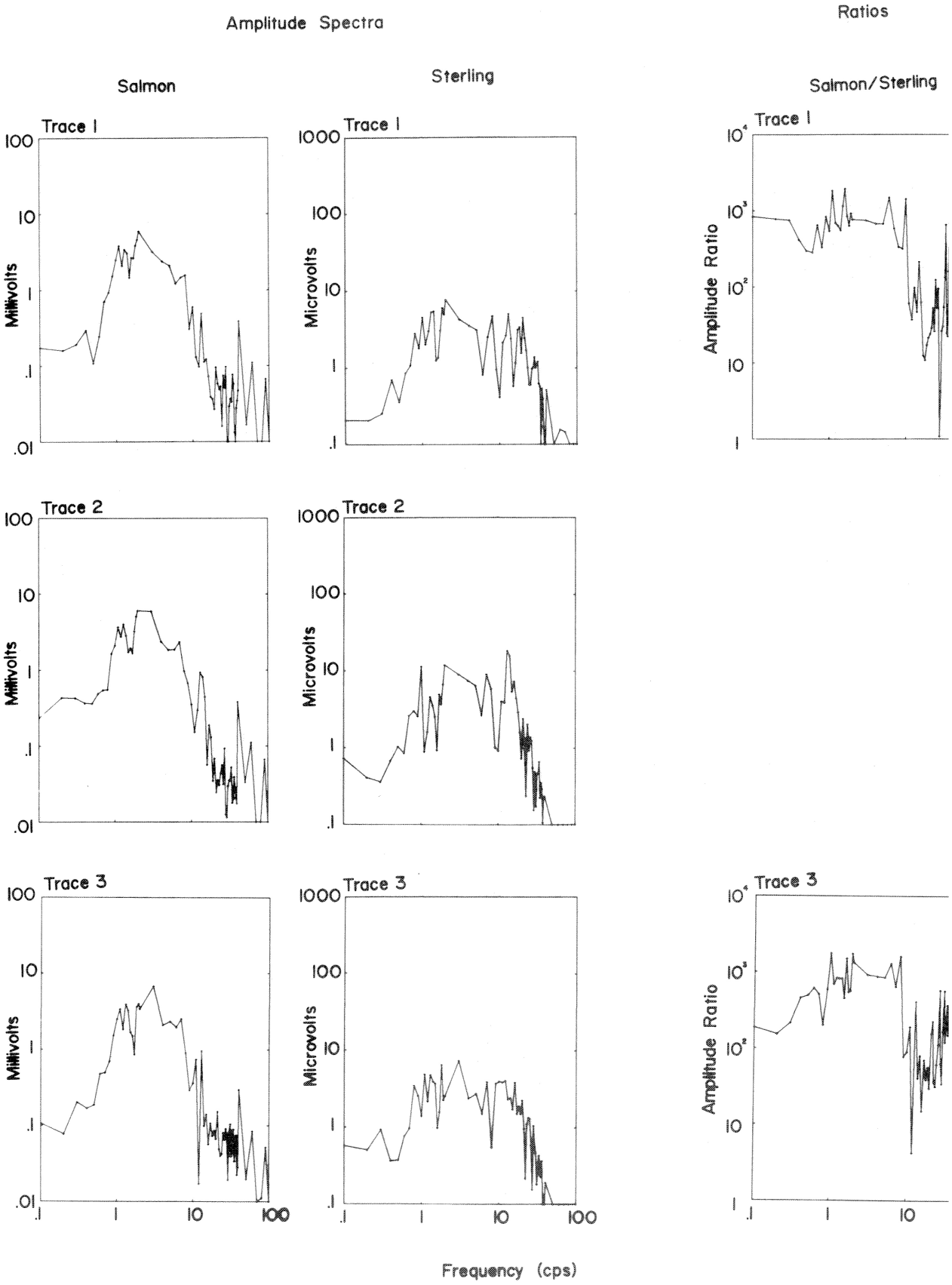
Amplitude Spectra
Ratios
Salmon
Sterling
Salmon/Sterling
Trace 1
Trace 2
Trace 3
Millivolts
Microvolts
Amplitude Ratio
100
10
1
.1
.01
1000
10^4
10^3
10^2
Frequency (cps)

Figure 21a

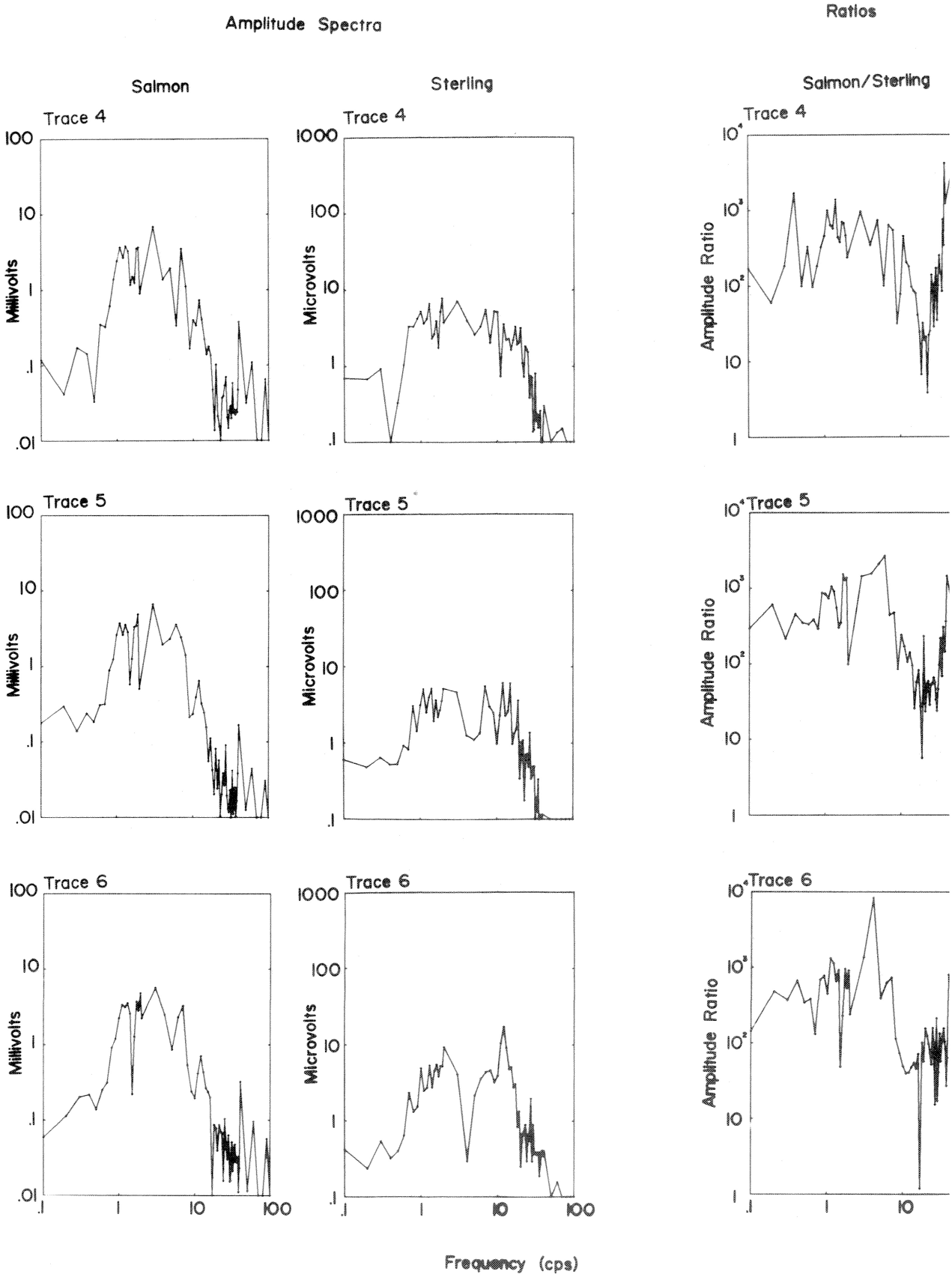
Amplitude Spectra
Ratios
Salmon
Sterling
Salmon/Sterling
Trace 4
Trace 5
Trace 6
Millivolts
Microvolts
Amplitude Ratio
Frequency (cps)

Figure 21b

Amplitude Spectra

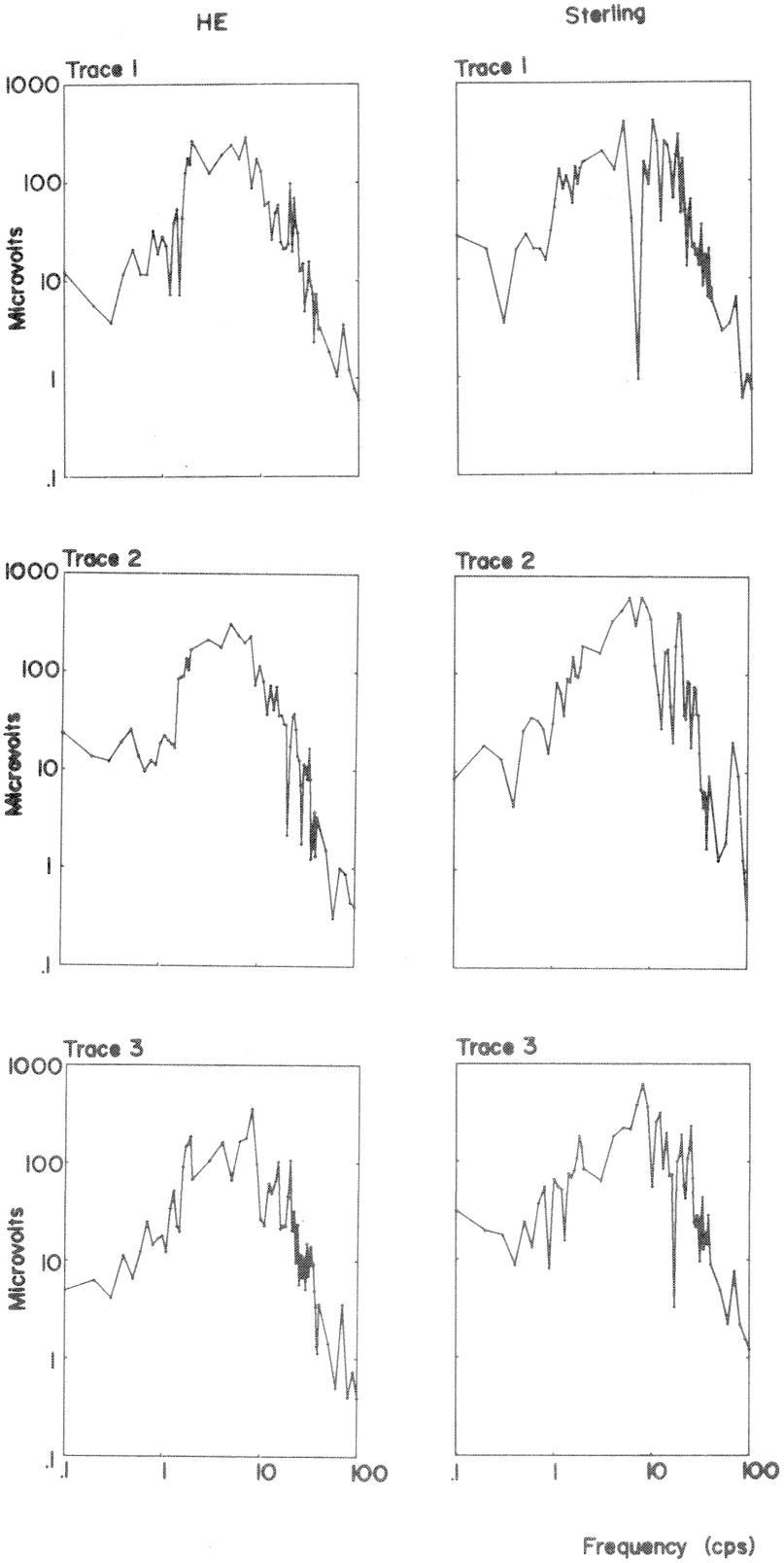

Figure 22a

Amplitude Spectra

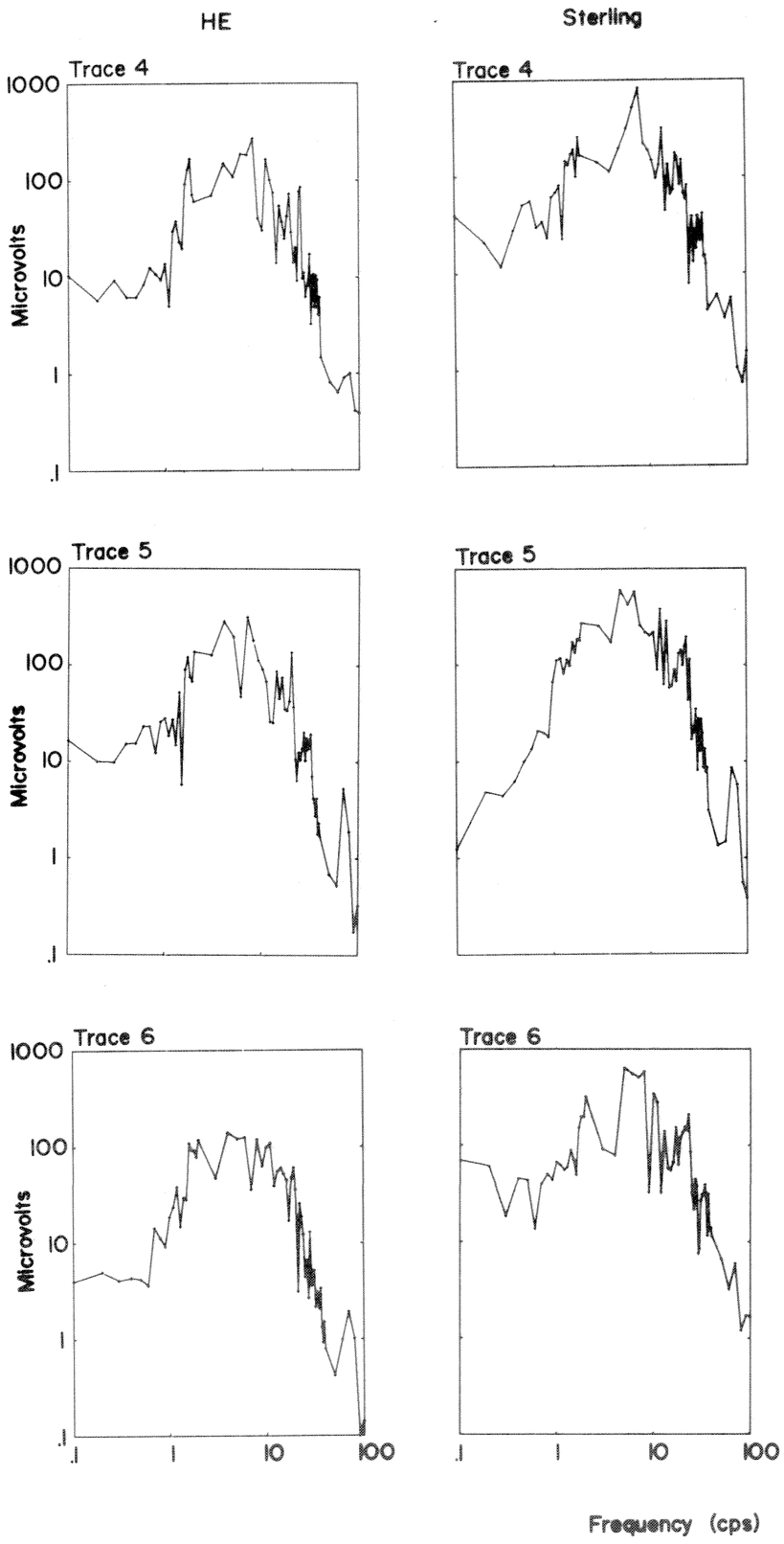

Figure 22b

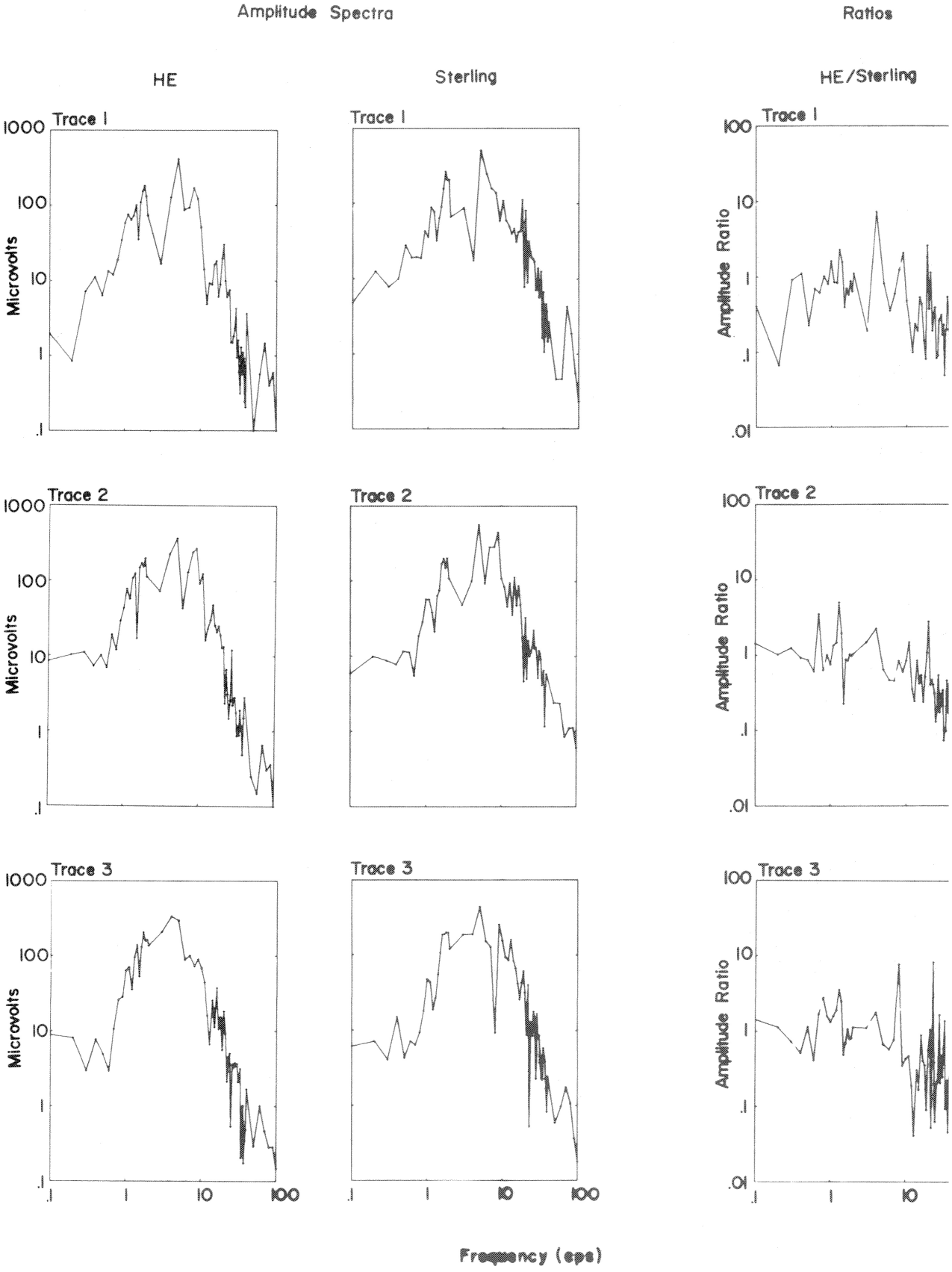
Amplitude Spectra
Ratios
HE
Sterling
HE/Sterling
Trace 1
Trace 2
Trace 3
Microvolts
Amplitude Ratio
1000
100
10
1
.1
.01
Frequency (cps)

Figure 23a

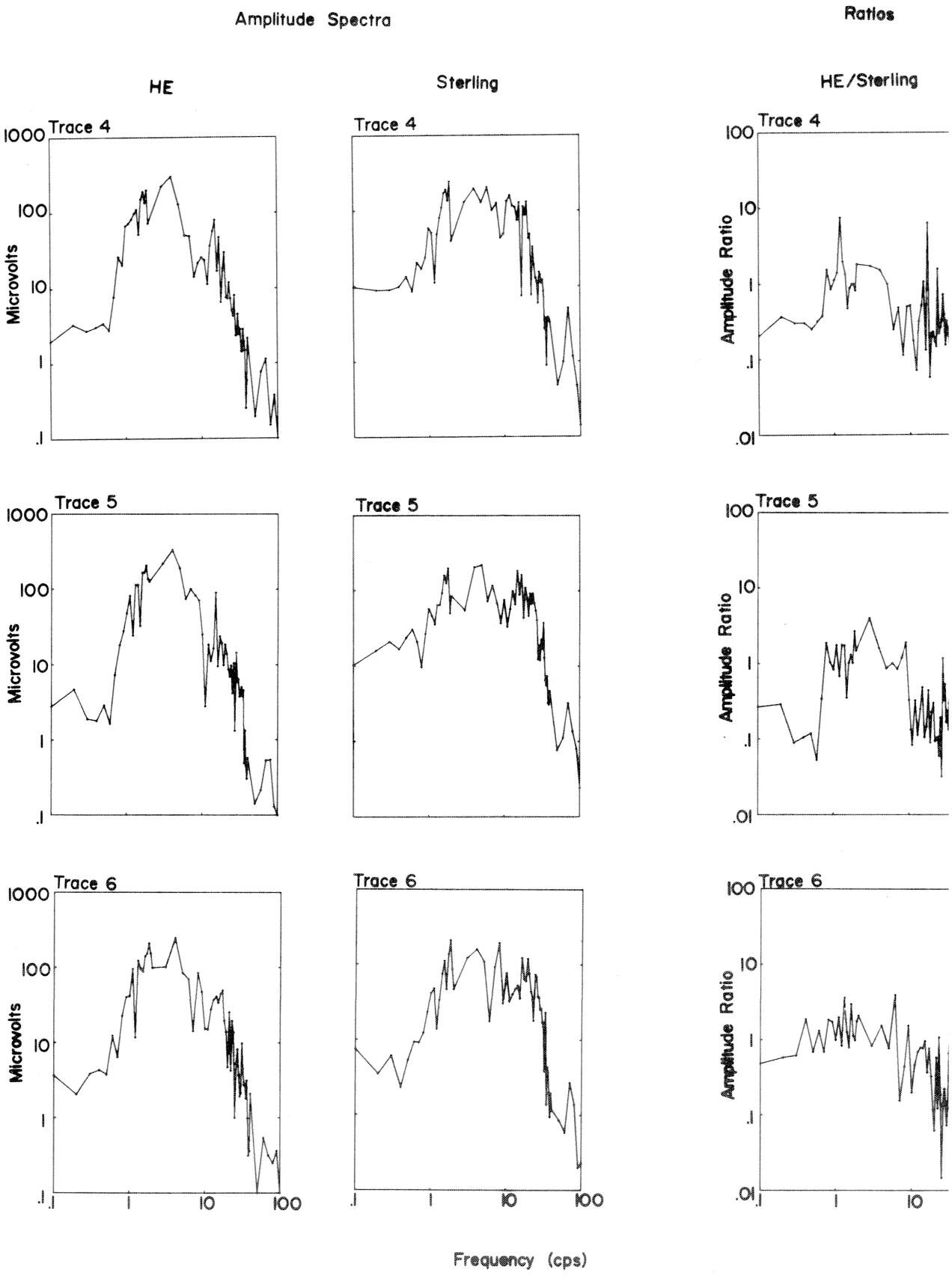
Amplitude Spectra
Ratios
HE
Sterling
HE/Sterling
Trace 4
Trace 5
Trace 6
Microvolts
Amplitude Ratio
1000
100
10
1
.1
.01
Frequency (cps)

Figure 23b

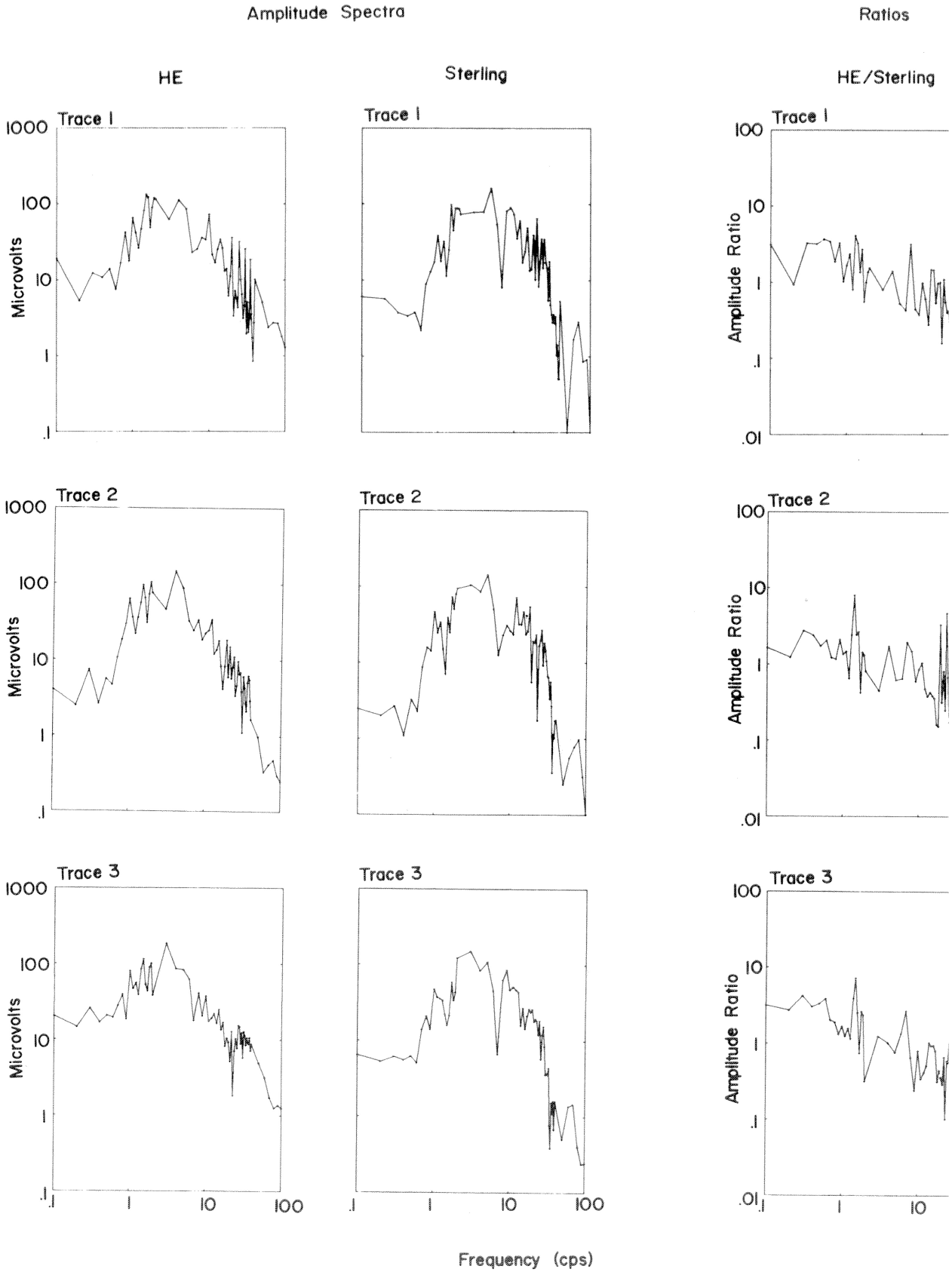

Figure 24a (Hotel)

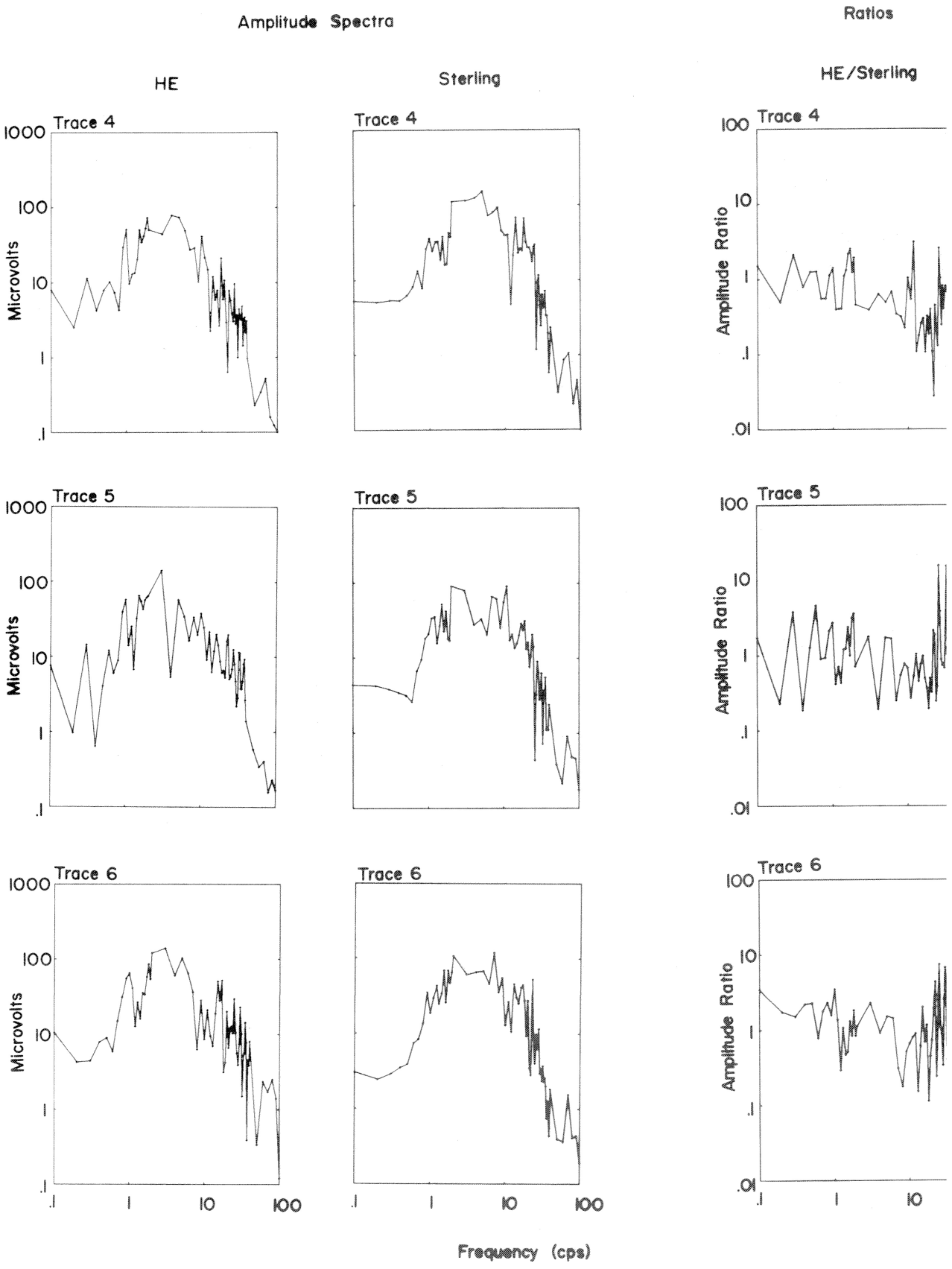

Figure 24b (Hotel)

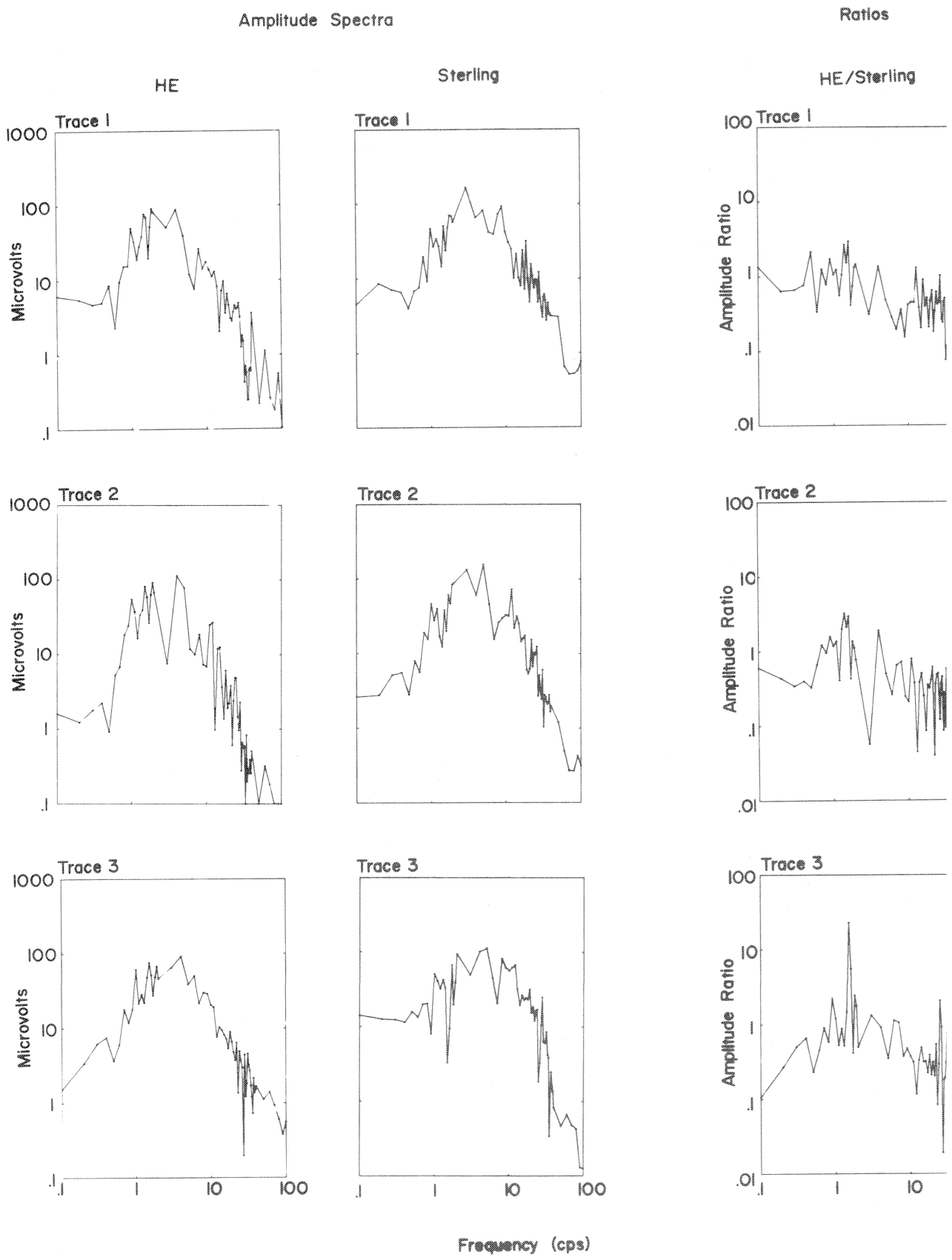

Figure 25a (Papa)

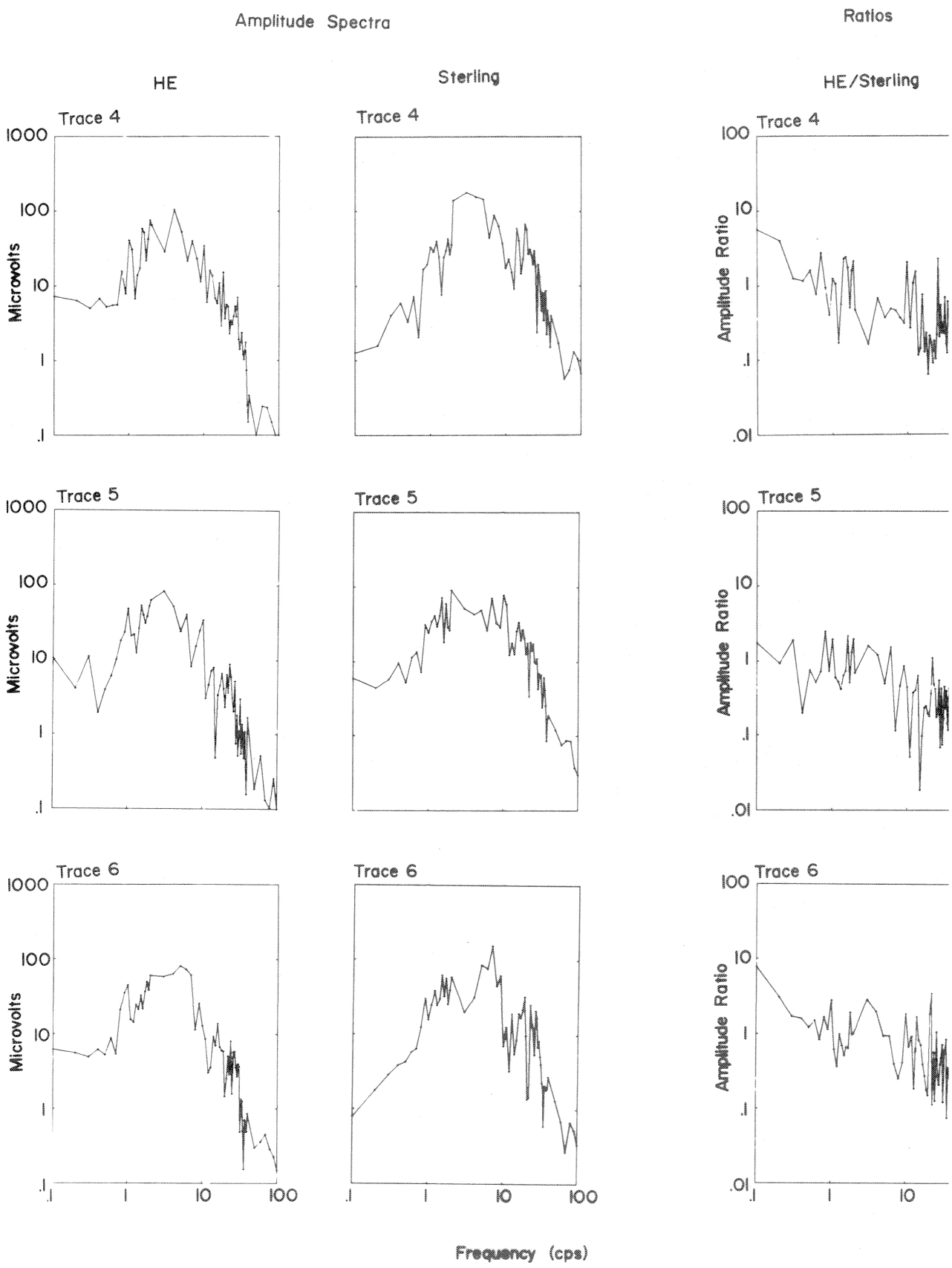

Figure 25b (Papa)

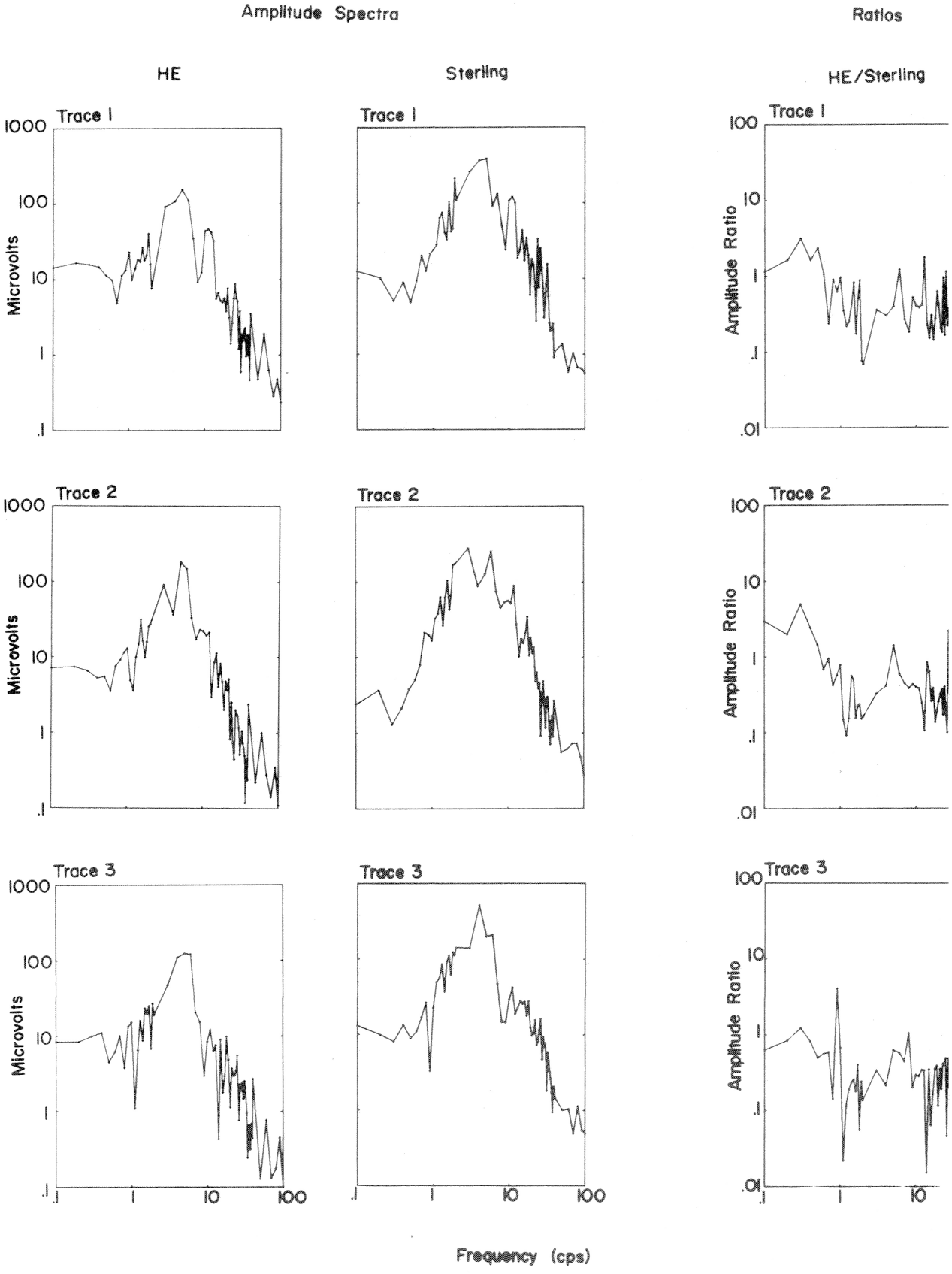
Amplitude Spectra
Ratios
HE
Sterling
HE/Sterling
Trace 1
Trace 2
Trace 3
Microvolts
Amplitude Ratio
1000
100
10
1
.1
.01
Frequency (cps)

Figure 26a

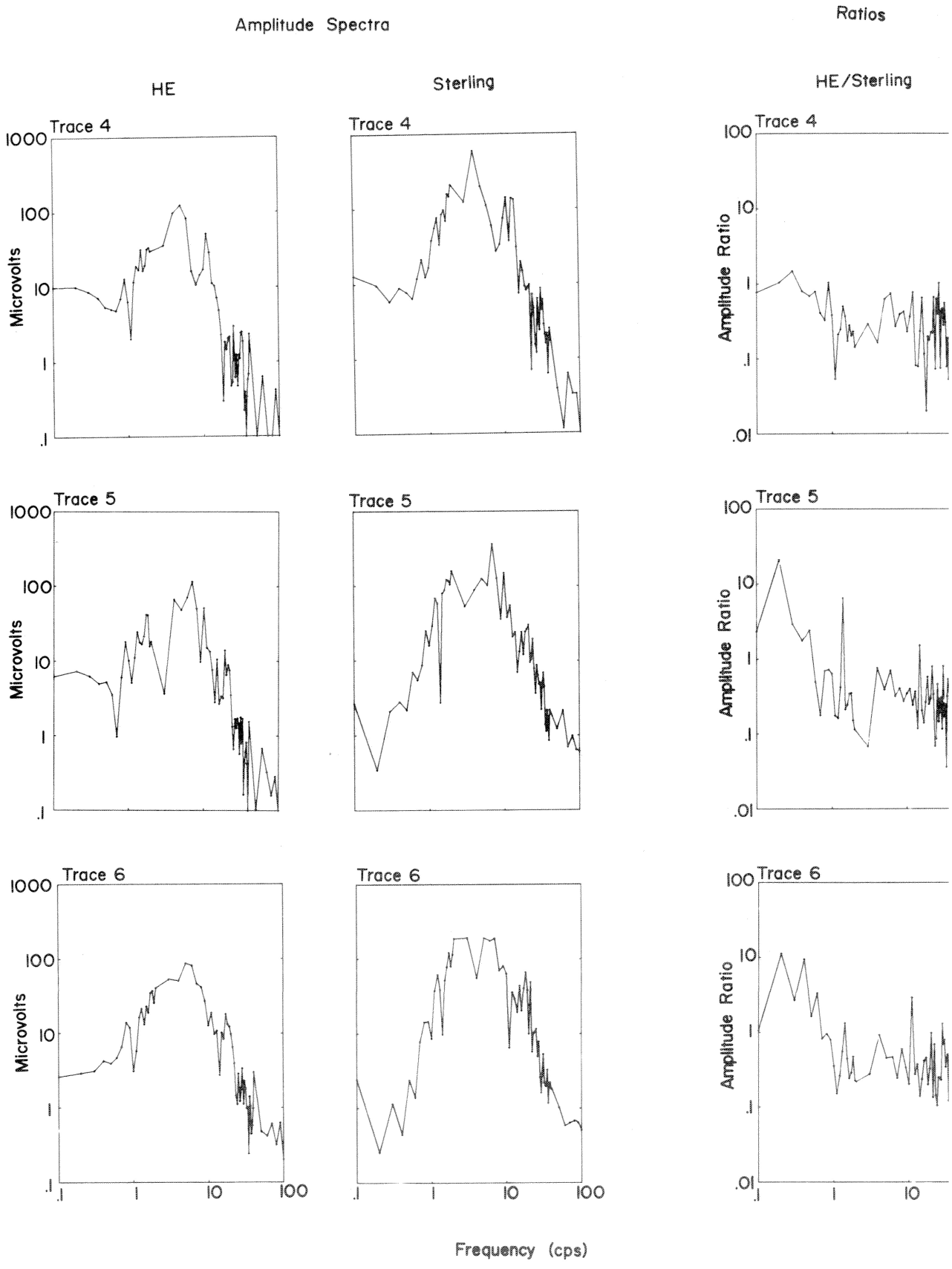
Amplitude Spectra
Ratios
HE
Sterling
HE/Sterling
Trace 4
Trace 5
Trace 6
Microvolts
Amplitude Ratio
1000
100
10
1
.1
.01
Frequency (cps)

Figure 26b

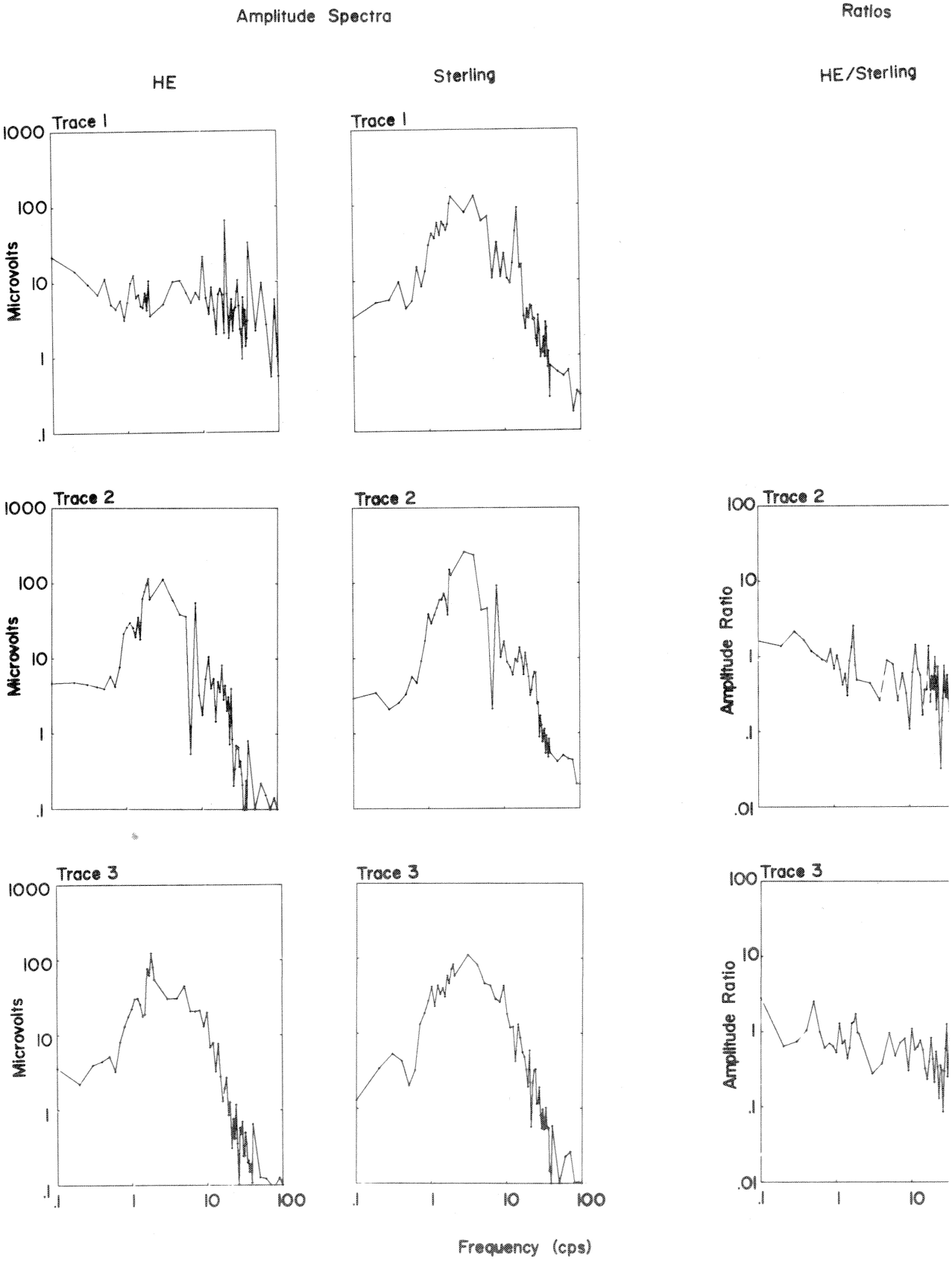
Amplitude Spectra
Ratios
HE
Sterling
HE/Sterling
Trace 1
Trace 2
Trace 3
Microvolts
Amplitude Ratio
1000
100
10
1
.1
.01
Frequency (cps)

Figure 27a

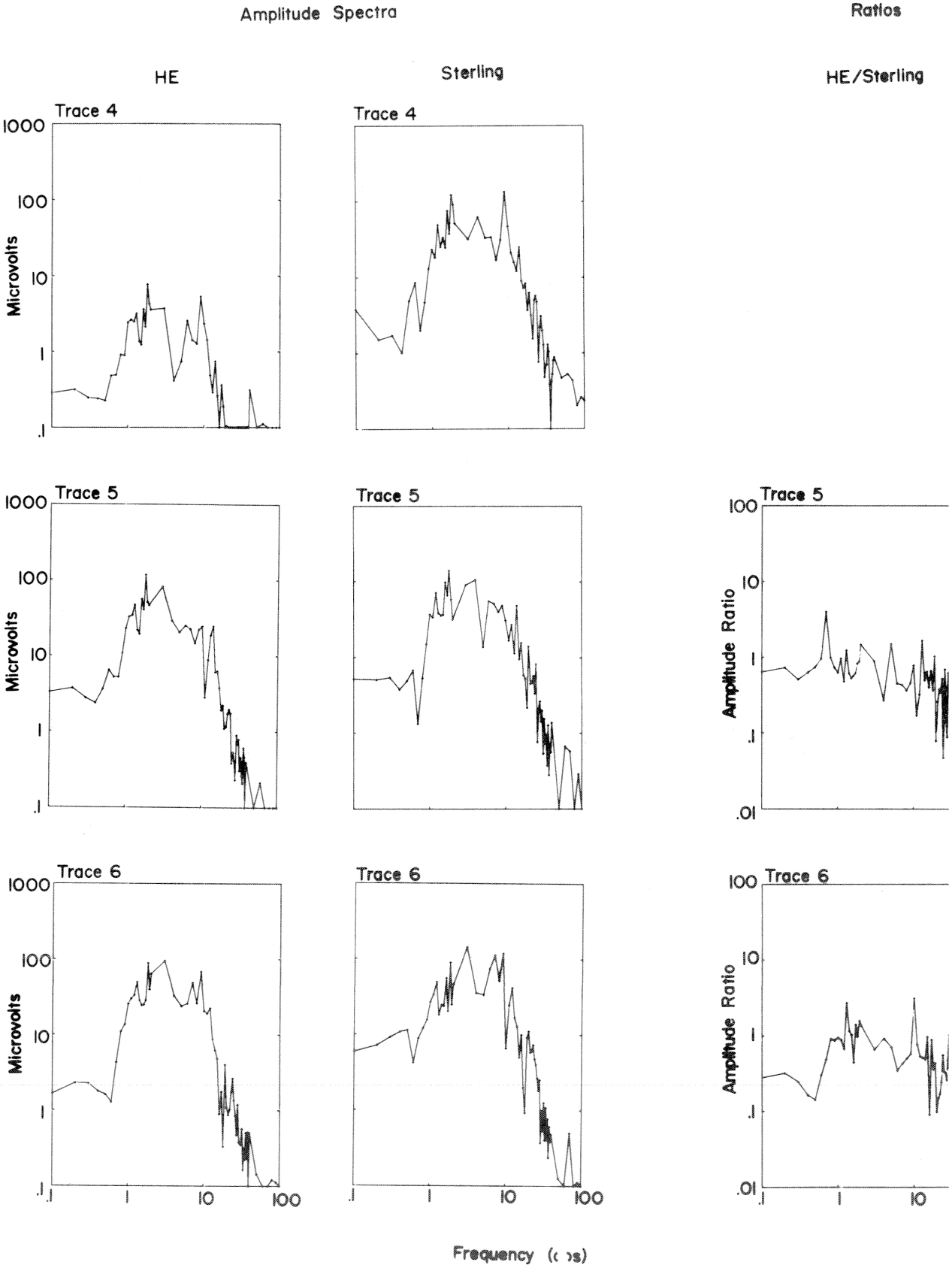
Amplitude Spectra
Ratios
HE
Sterling
HE/Sterling
Trace 4
Trace 5
Trace 6
Microvolts
Amplitude Ratio
1000
100
10
1
.1
.01
Frequency (c/s)

Figure 27b

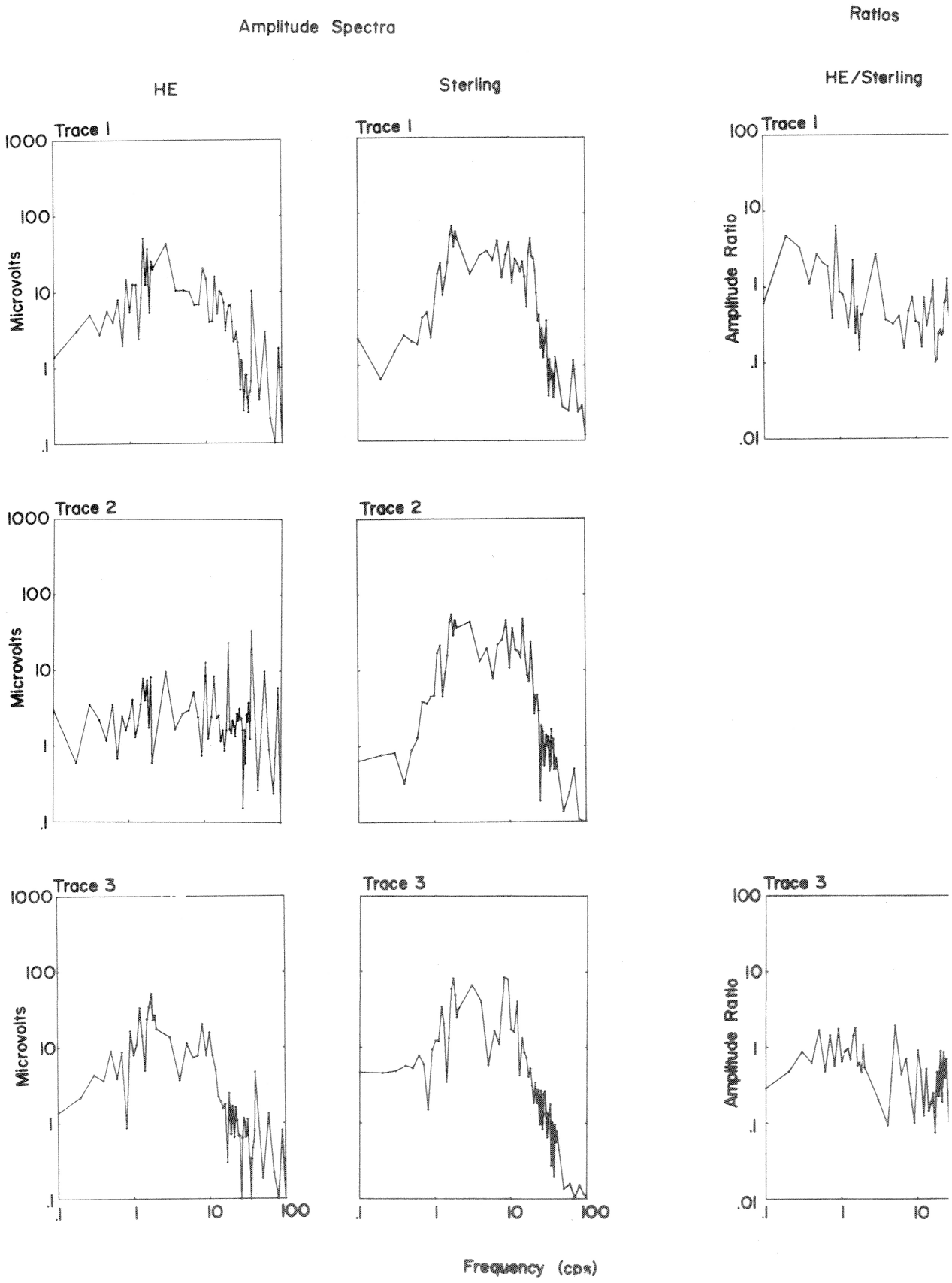
Amplitude Spectra
Ratios
HE
Sterling
HE/Sterling
Trace 1
Trace 2
Trace 3
Microvolts
Amplitude Ratio
1000
100
10
1
.1
.01
Frequency (cps)

Figure 28a

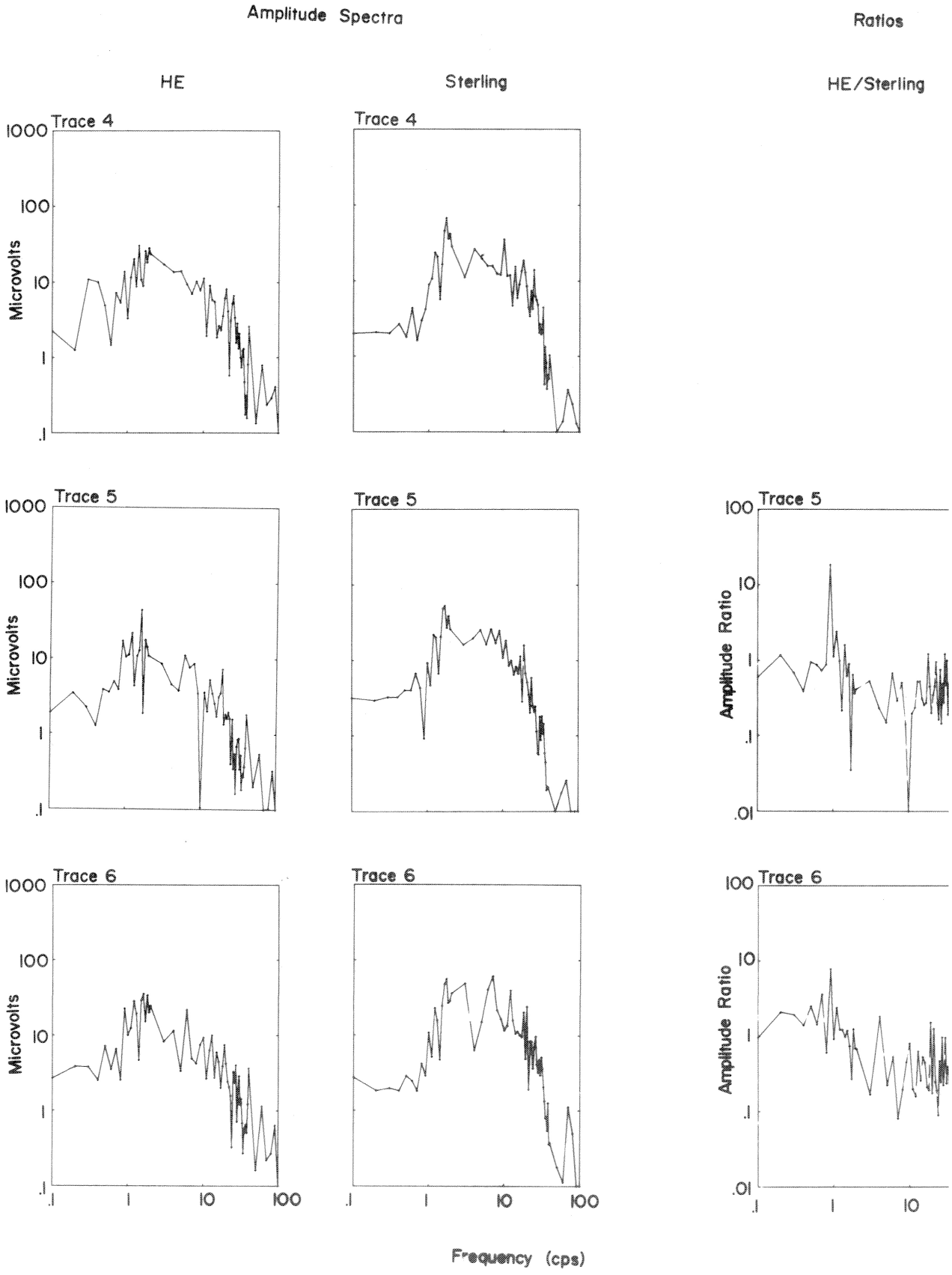
Amplitude Spectra
Ratios
HE
Sterling
HE/Sterling
Trace 4
Trace 5
Trace 6
Microvolts
Amplitude Ratio
1000
100
10
1
.1
.01
Frequency (cps)

Figure 28b

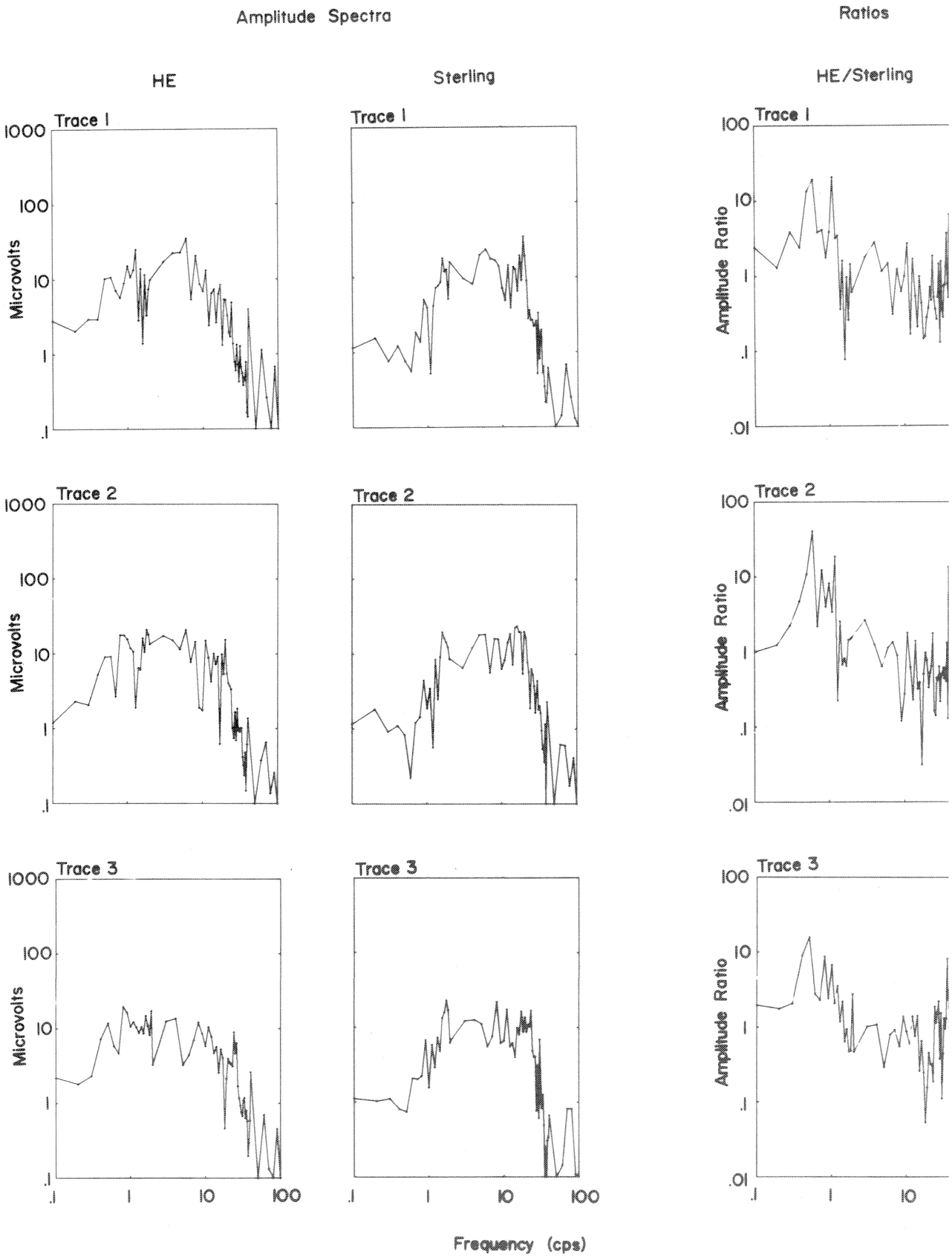
Amplitude Spectra
Ratios
HE
Sterling
HE/Sterling
Trace 1
Trace 2
Trace 3
Microvolts
Amplitude Ratio
1000
100
10
1
.1
.01
Frequency (cps)

Figure 29a

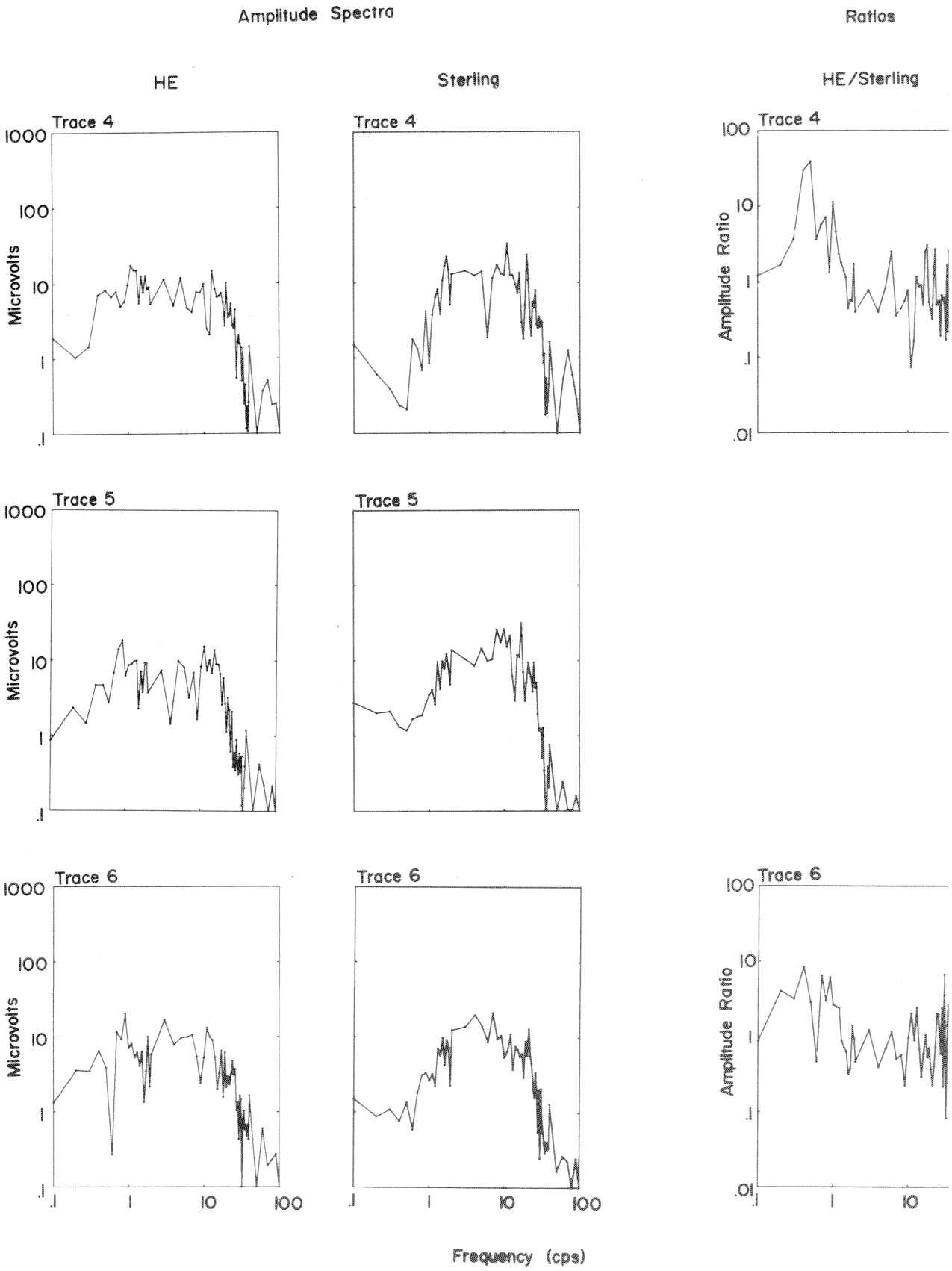
Amplitude Spectra
Ratios
HE
Sterling
HE/Sterling
Trace 4
Trace 5
Trace 6
Microvolts
Amplitude Ratio
1000
100
10
1
.1
.01
Frequency (cps)

Figure 29b

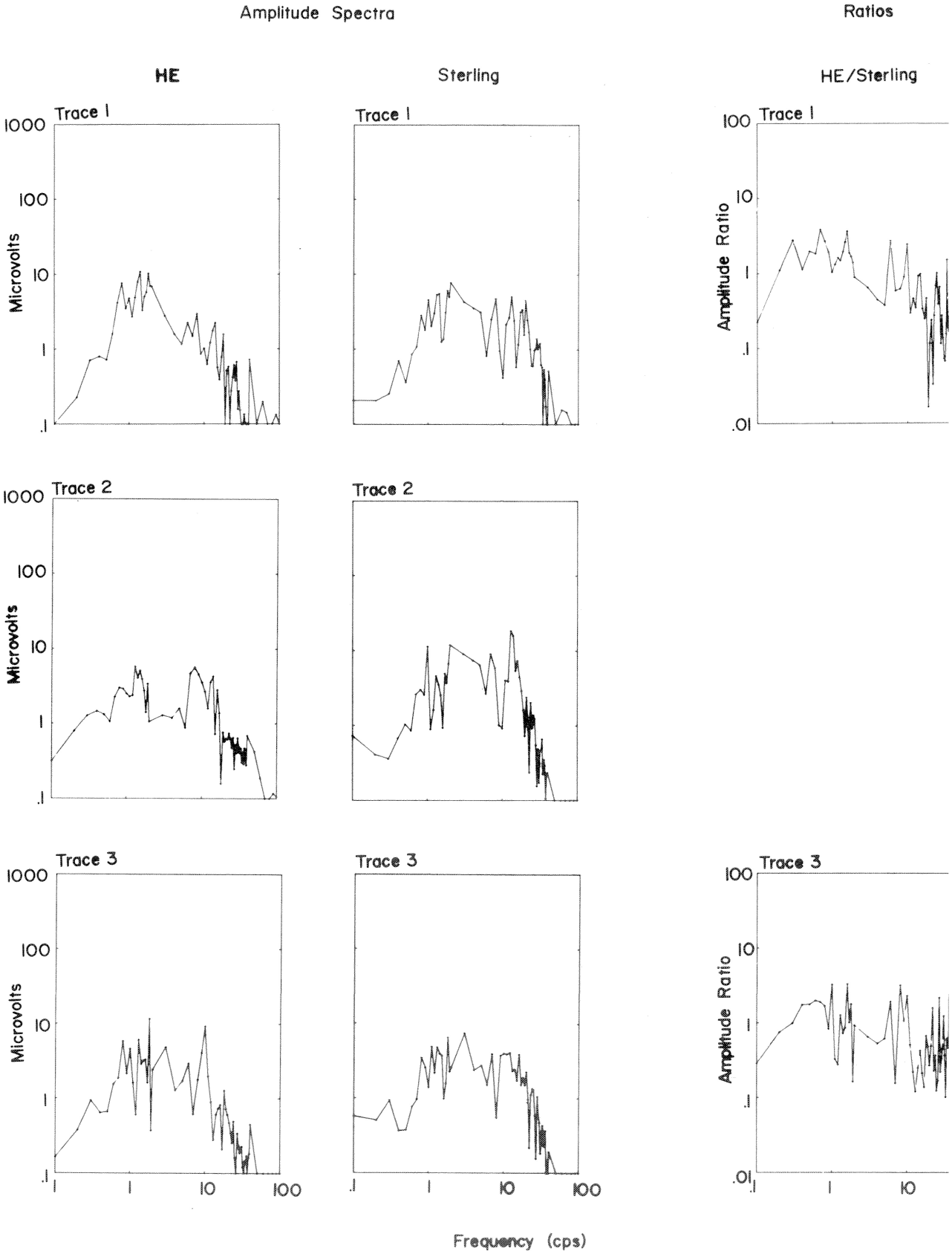
Amplitude Spectra
Ratios
HE
Sterling
HE/Sterling
Trace 1
Trace 2
Trace 3
Microvolts
Amplitude Ratio
1000
100
10
1
.1
.01
Frequency (cps)

Figure 30a

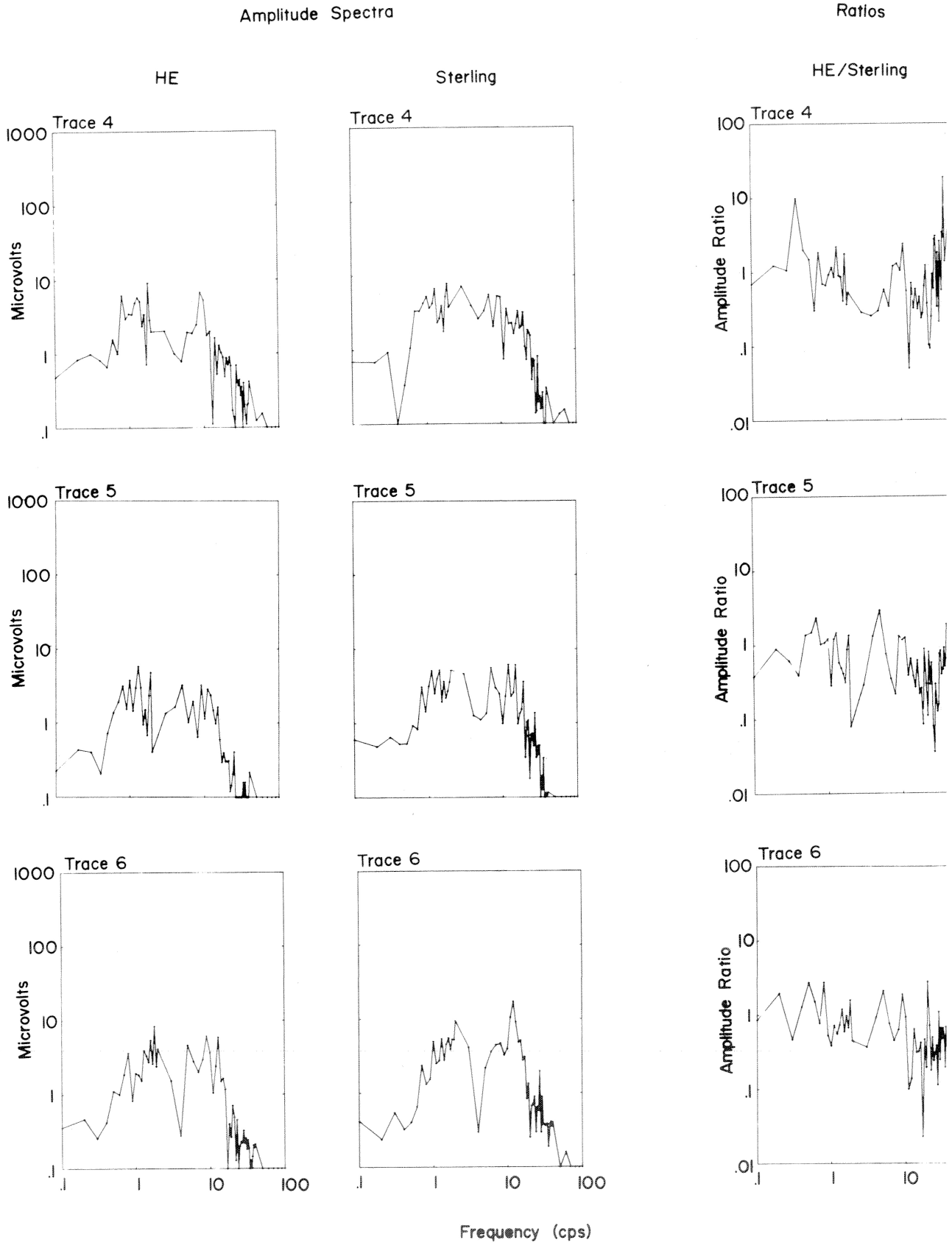
Amplitude Spectra
Ratios
HE
Sterling
HE/Sterling
Trace 4
Trace 5
Trace 6
Microvolts
Amplitude Ratio
1000
100
10
1
.1
.01
Frequency (cps)

Figure 30b

Noise Amplitude Spectra

Salmon

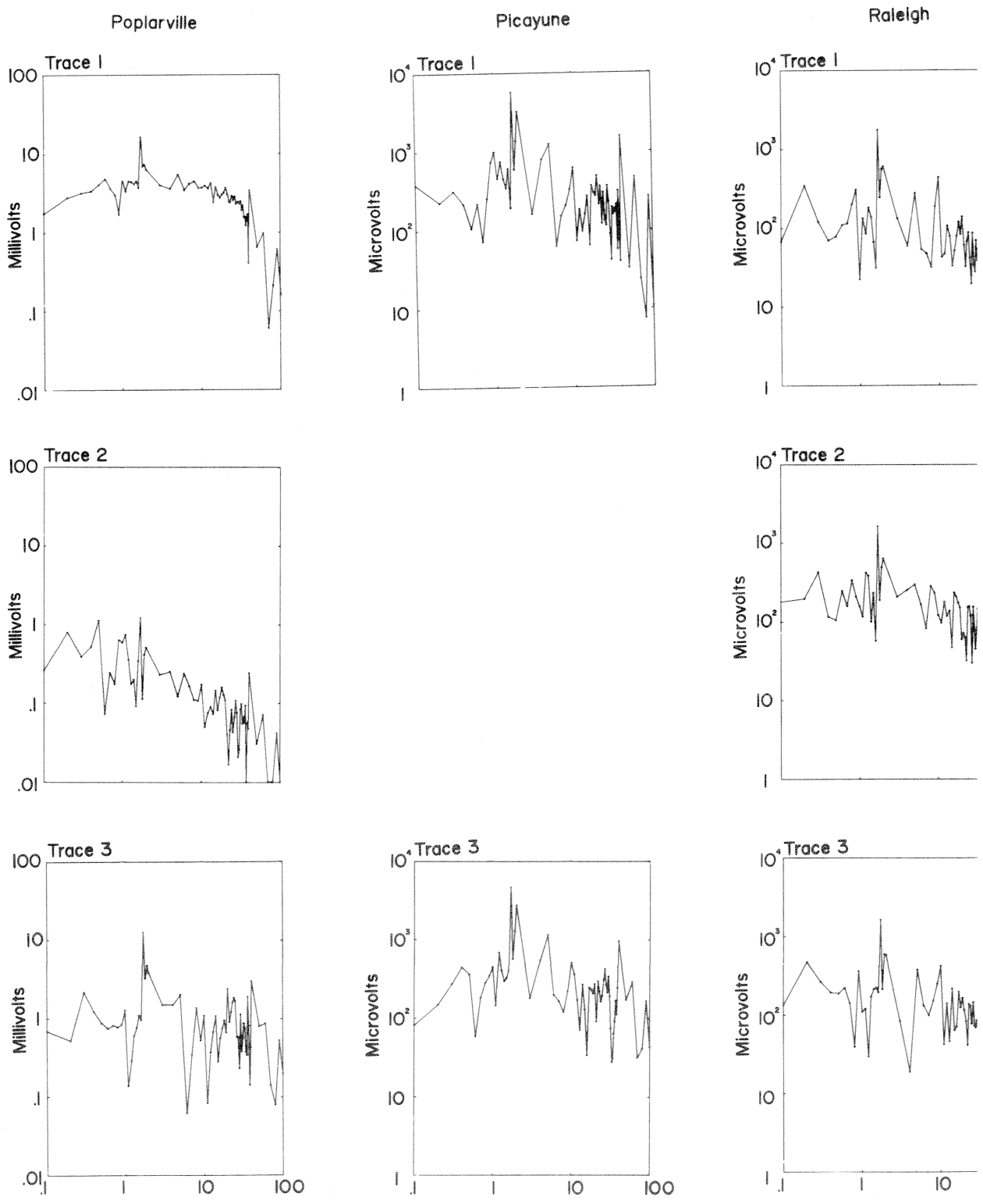

Figure 31a

Noise Amplitude Spectra

Salmon

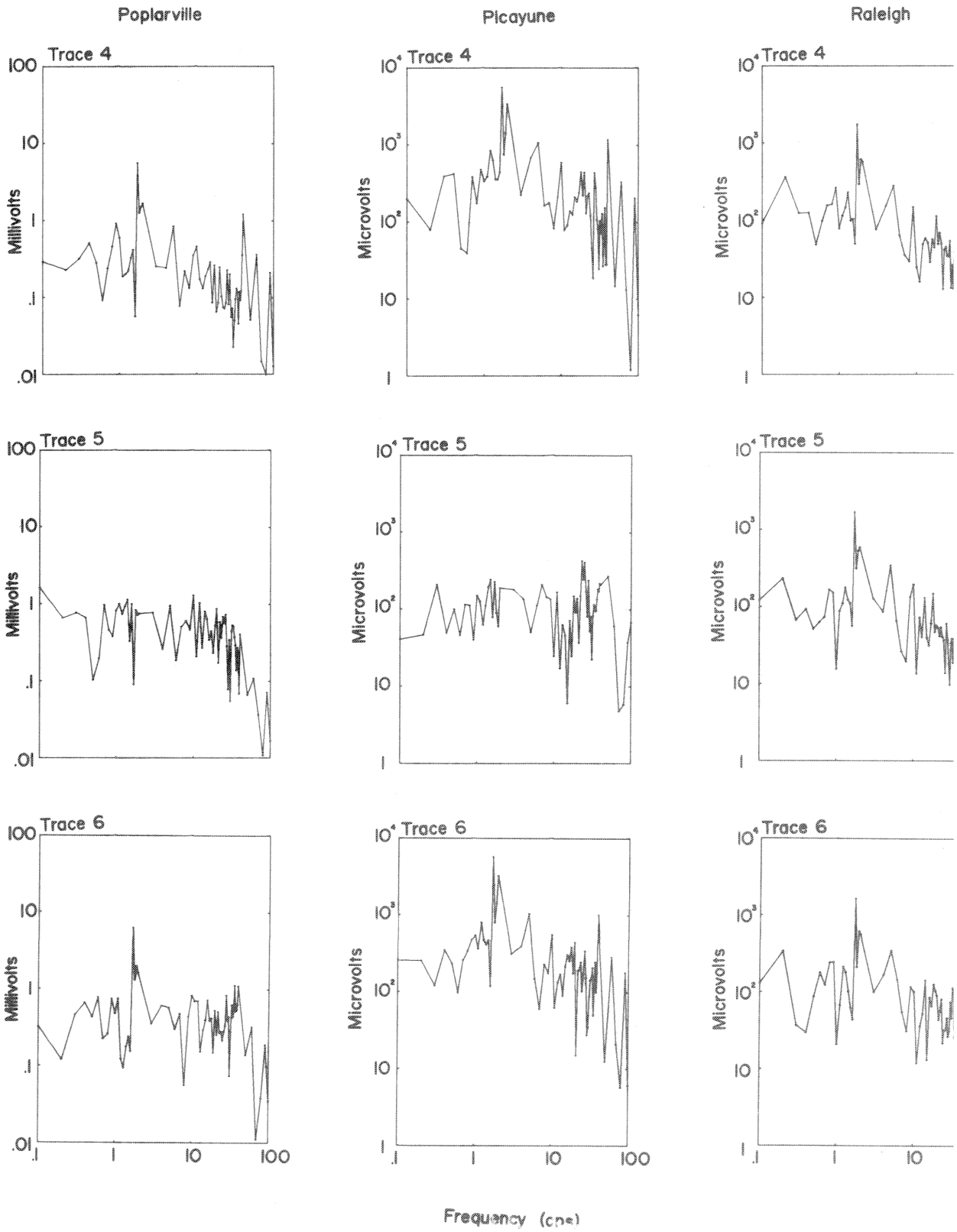

Figure 31b

Noise Amplitude Spectra

Sterling

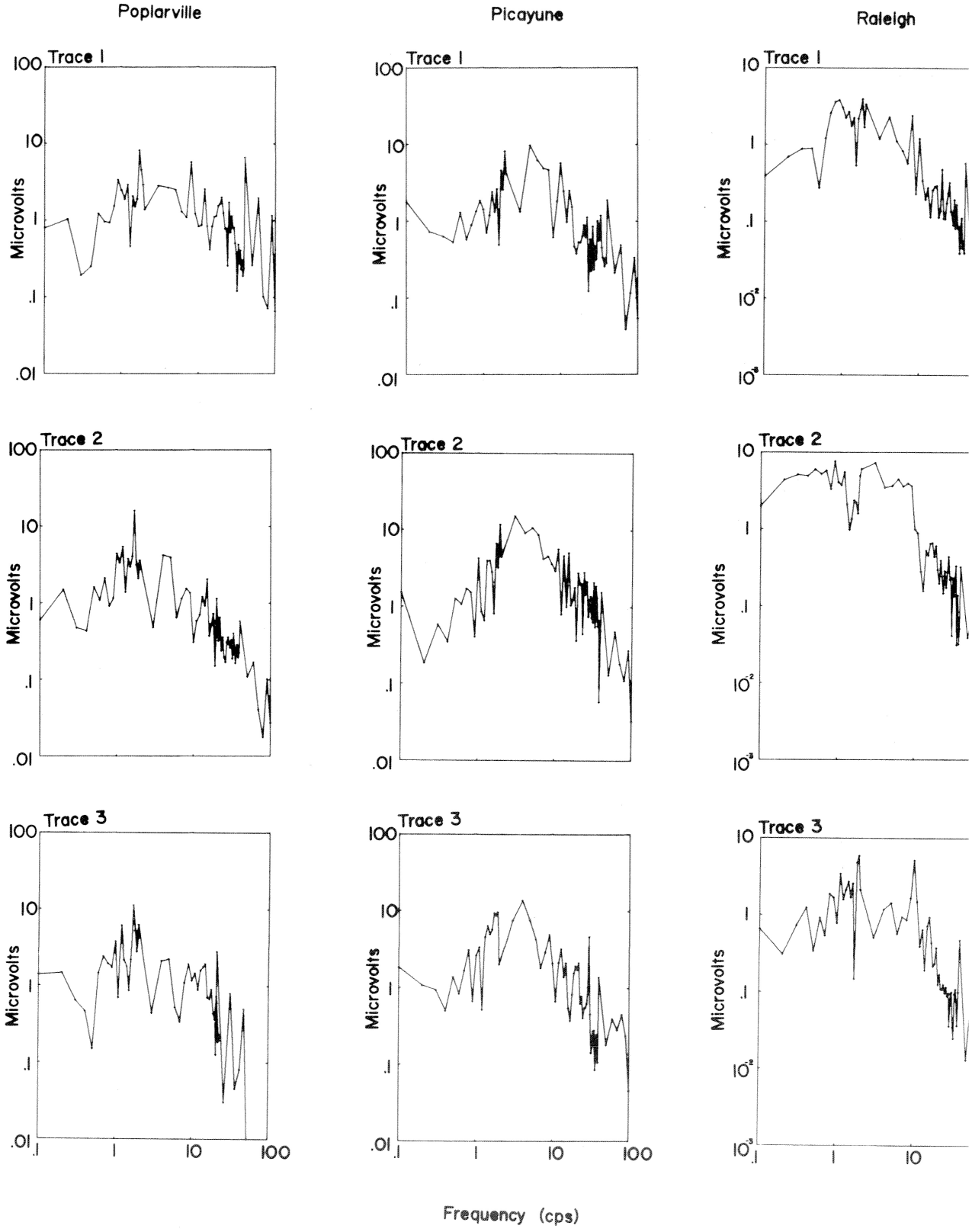

Figure 32a

Noise Amplitude Spectra

Sterling

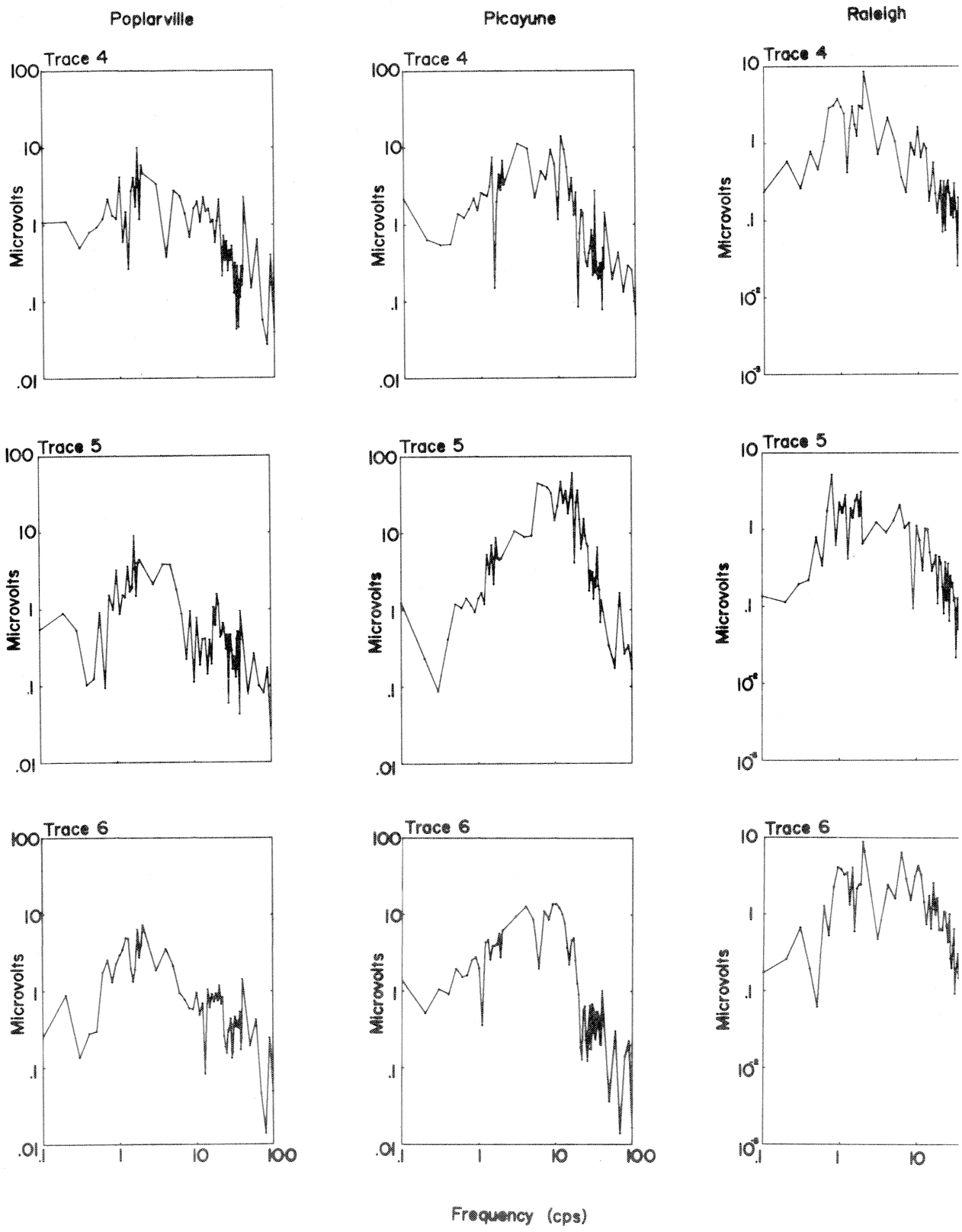

Figure 32b

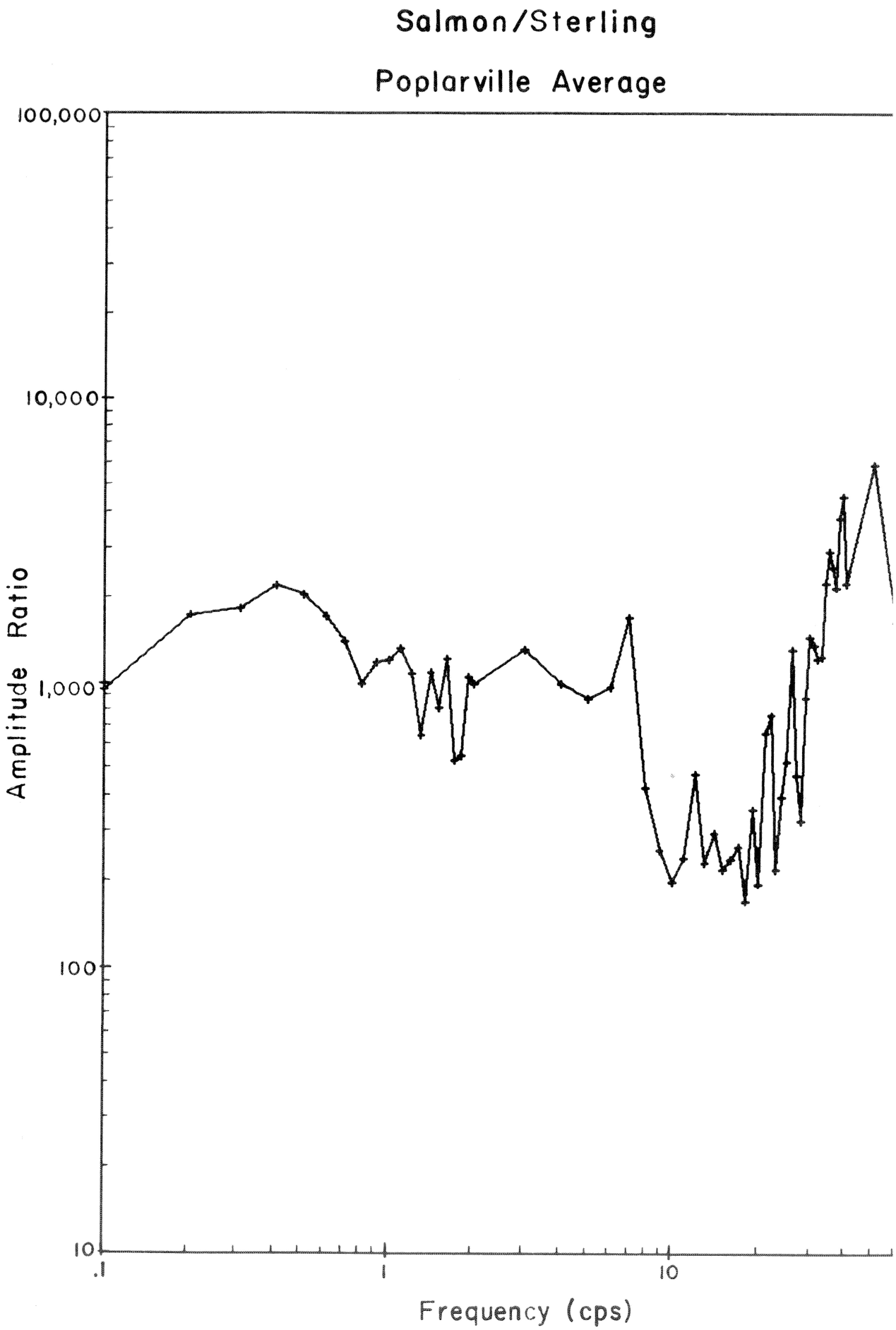
Salmon/Sterling
Poplarville Average
100,000
10,000
1,000
100
10
Amplitude Ratio
.1
1
10
Frequency (cps)

Figure 33

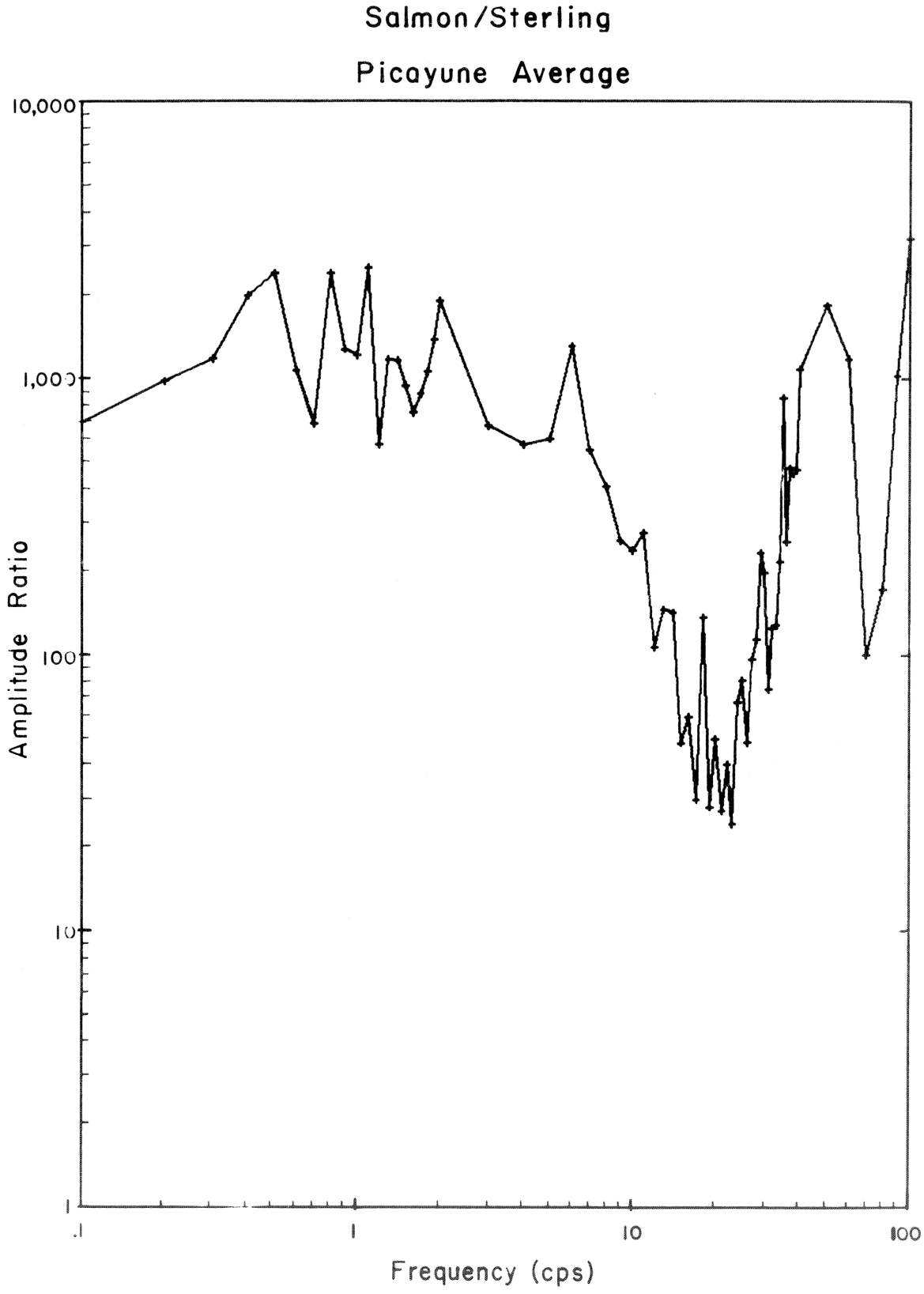
Salmon/Sterling
Picayune Average
10,000
1,000
100
10
1
Amplitude Ratio
.1
1
10
100
Frequency (cps)

Figure 34

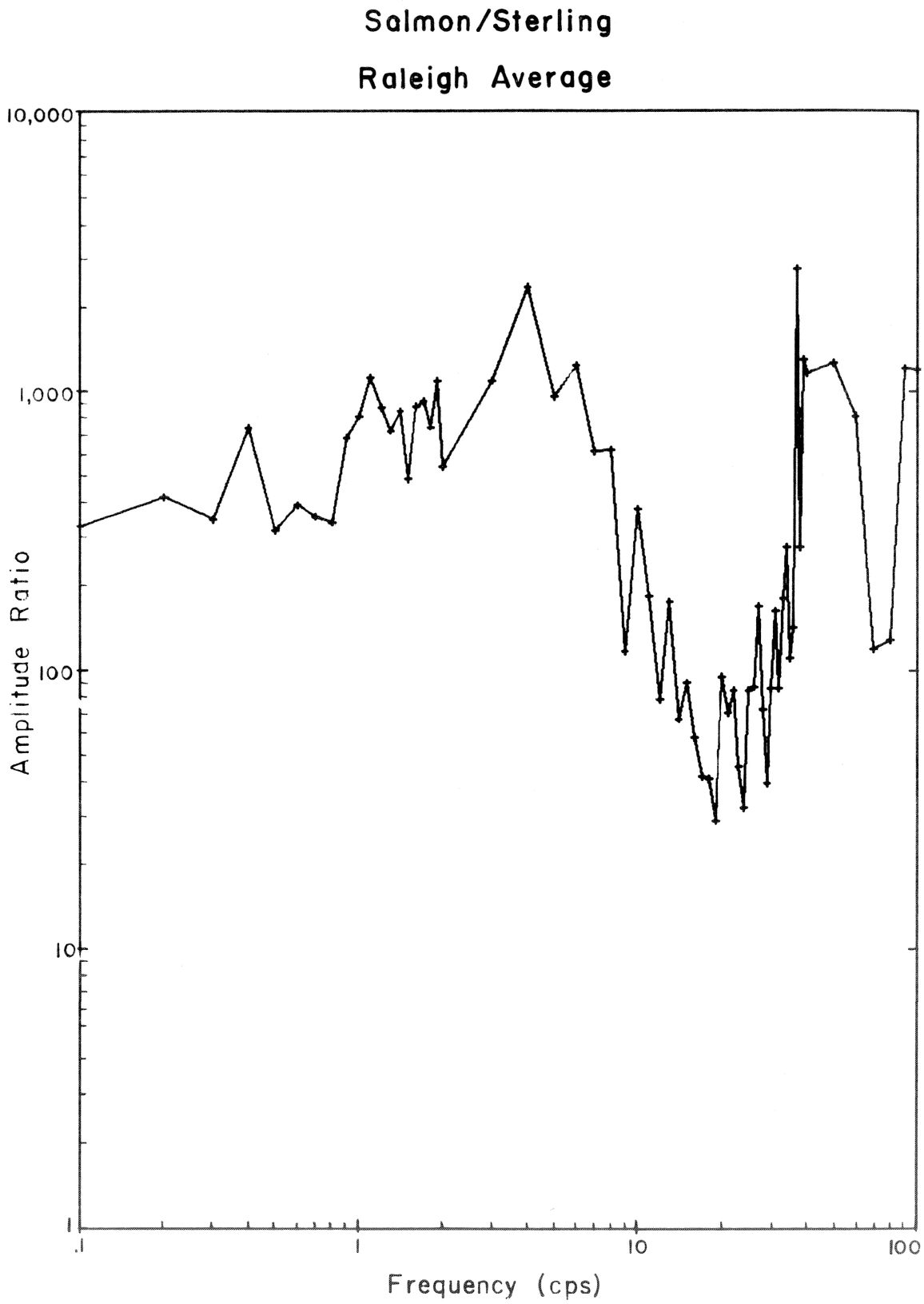
Salmon/Sterling
Raleigh Average
10,000
1,000
100
10
1
Amplitude Ratio
.1
1
10
100
Frequency (cps)

Figure 25

Average Amplitude Ratios

HE/Sterling

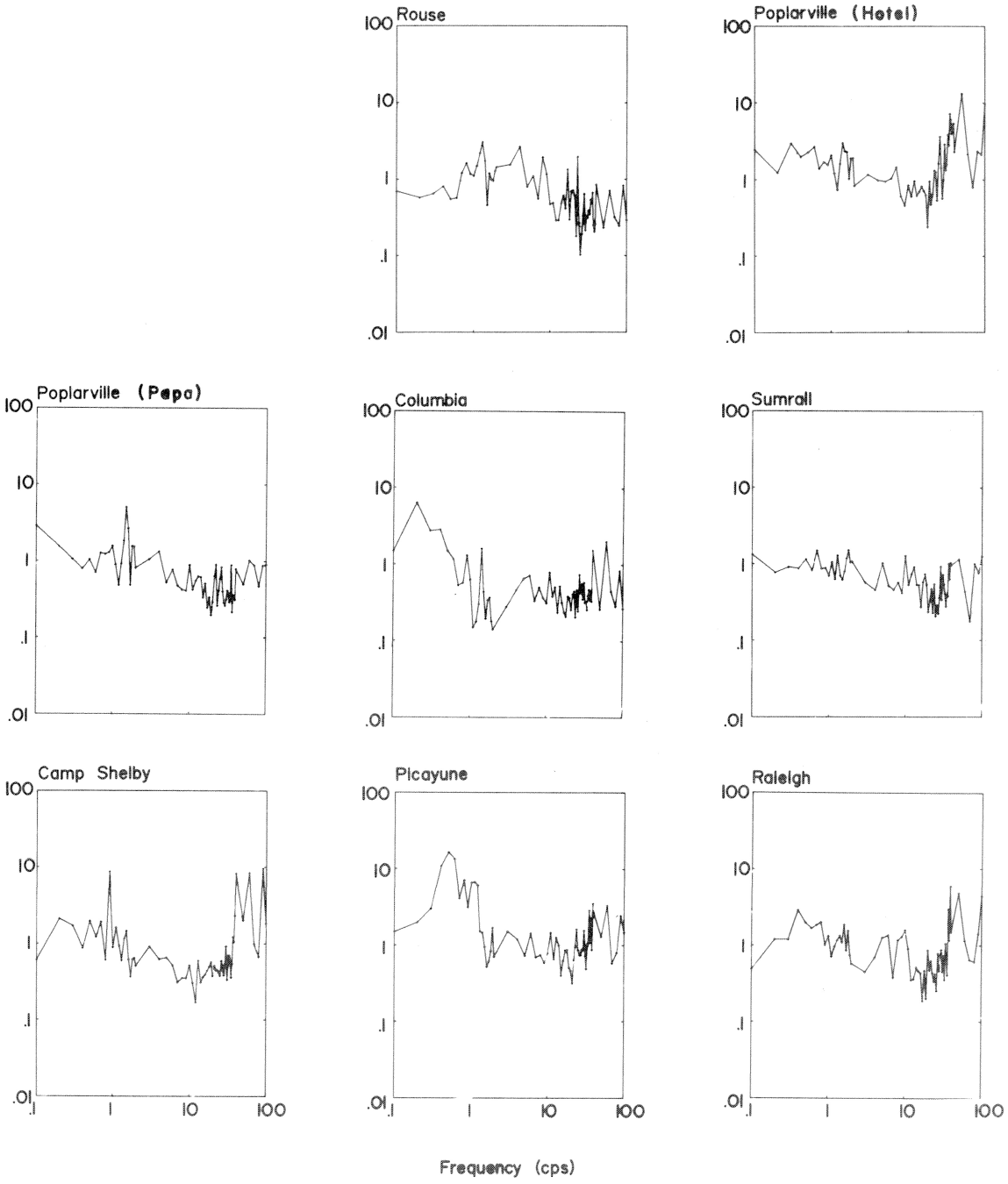

Figure 36

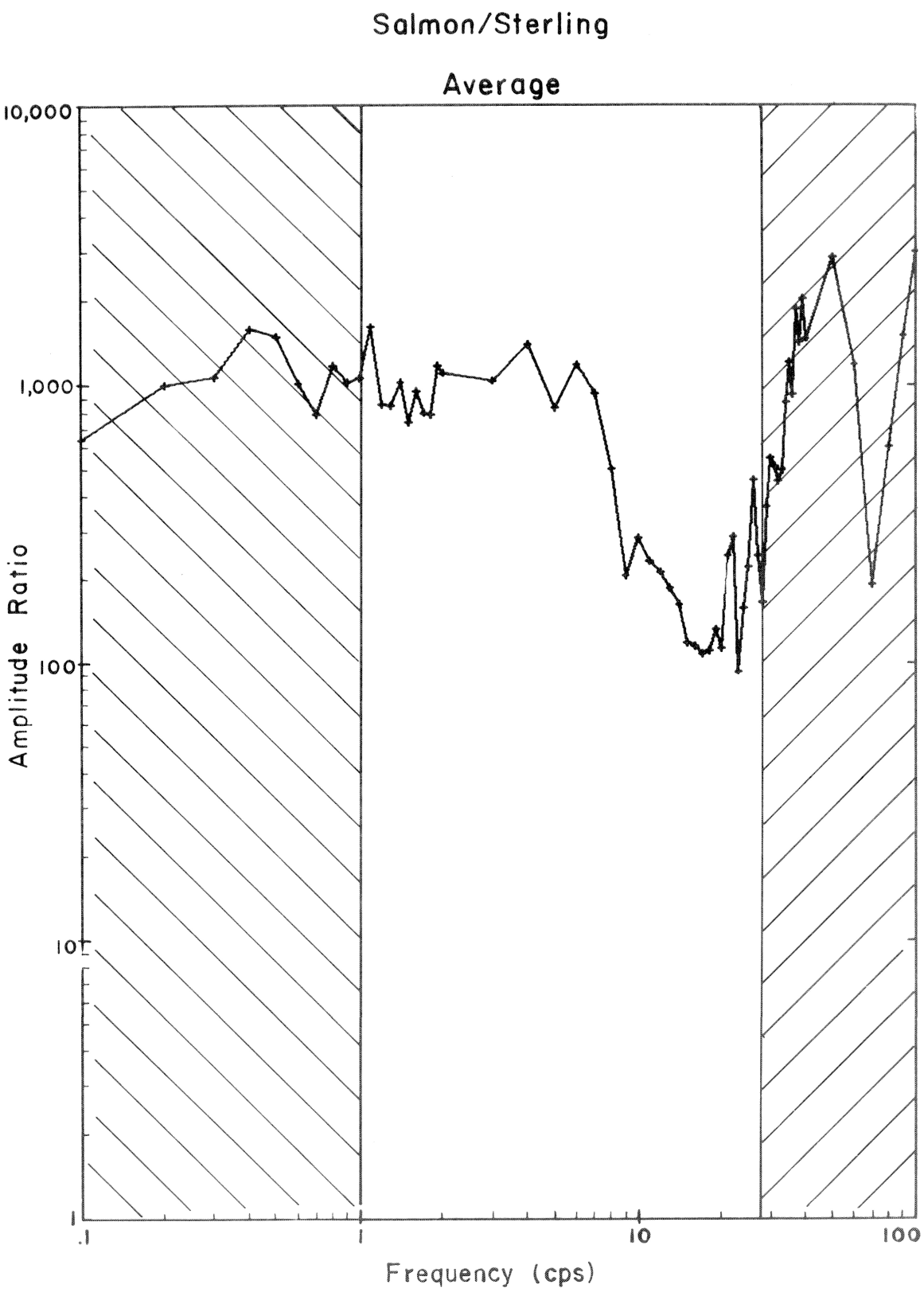
Salmon/Sterling
Average
10,000
1,000
100
10
1
Amplitude Ratio
.1
1
10
100
Frequency (cps)

Figure 37

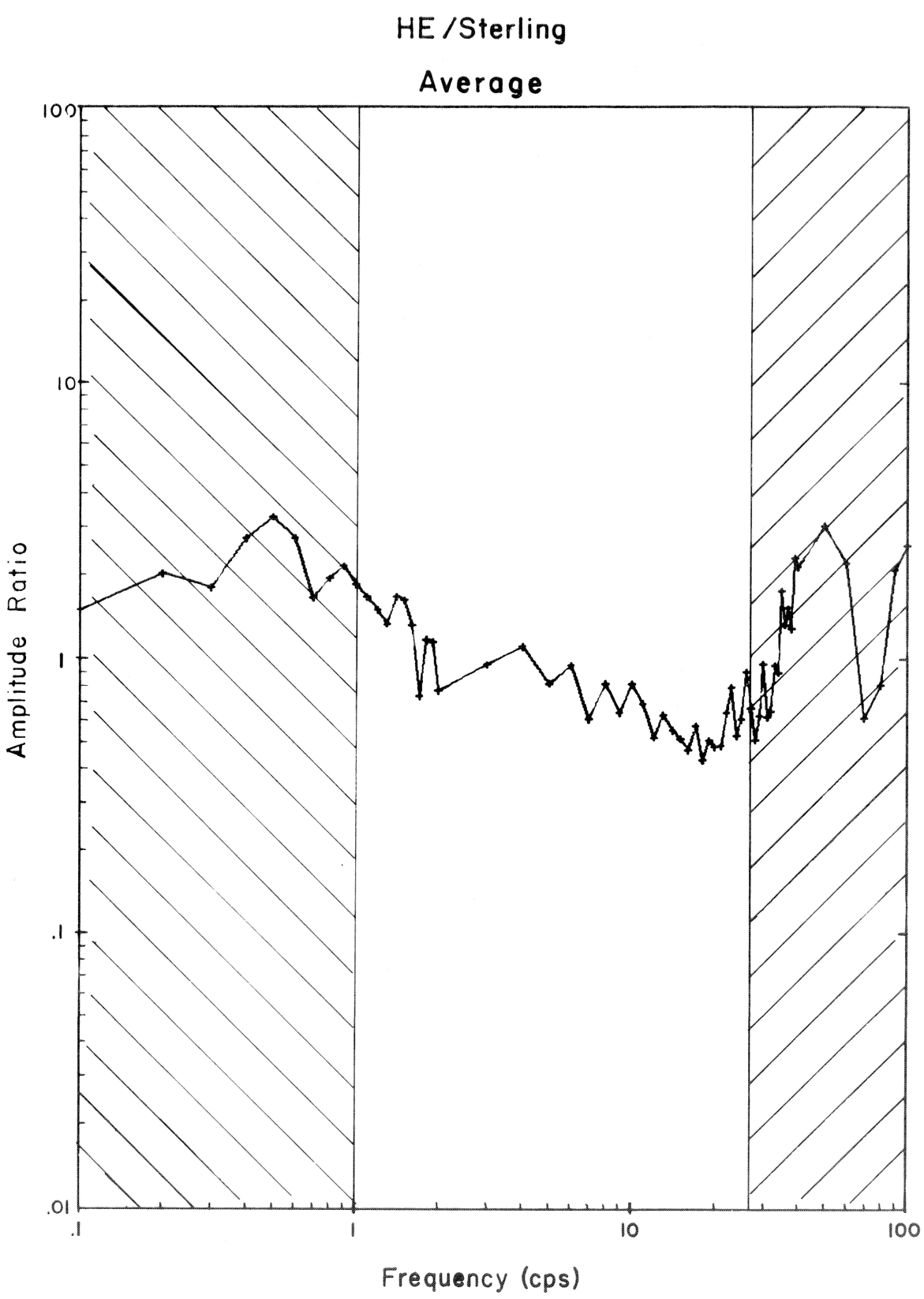
HE/Sterling
Average
100
10
1
.1
.01
Amplitude Ratio
.1
1
10
100
Frequency (cps)

Figure 38